Annu. Rev. Astron. Astrophys. 1991. 29: 581–625

MOLECULAR GAS IN GALAXIES

J. S. Young

Department of Physics and Astronomy and Five College Radio Astronomy Observatory, University of Massachusetts, Amherst, Massachusetts 01003

N. Z. Scoville

Astronomy Department, California Institute of Technology 105-24, Pasadena, California 91125

KEY WORDS: star formation, Hubble sequence, galaxy evolution, interstellar medium

1. INTRODUCTION

Molecular gas is critical in determining both the morphology and evolution of galactic disks. It is within the giant molecular clouds that interstellar gas is cycled into the next generation of stars, and the most massive of these young stars produce a major part of the galactic luminosity. In addition, the dense interstellar medium, as it is highly dissipative, probably plays a fundamental part in determining the outcome of galactic interactions. Over the last two decades, CO observations have been used to probe the molecular component of hundreds of galaxies from the Local Group to the Virgo cluster, and in luminous galaxies with recession velocities up to $cz = 45{,}000$ km s^{-1}.

The studies of molecules in galaxies include both detailed analyses of nearby galaxies and comparisons of the global properties of selected samples of galaxies. These two approaches are complementary, and both are necessary to improve our understanding of the large-scale processes that govern star formation and molecular cloud evolution. The CO observations are now sufficient to address statistically the global H_2 content of galaxies in relation to other components of the interstellar medium (ISM) and the stellar populations, as a function of morphological type, lumi-

0066-4146/91/0915-0581$02.00

nosity, and environment. Specifically:

1. What is the range of H_2 masses in galaxies, and is there a dependence on galaxy type, luminosity, or environment?
2. What is the ratio L_*/M_{gas}, or the yield of young stars per unit mass of gas (i.e. the star formation efficiency), within individual galaxies and from galaxy to galaxy?
3. What is the range of $M(H_2)/M(H\,I)$ in galaxies, and is there a dependence on galaxy type, luminosity, or environment?
4. What are the effects of spiral arms on the multiphase interstellar gas and the formation of stars?
5. What is the role of the molecular gas component in galactic interactions, starburst galaxies, and active galaxy nuclei?

The answers to these questions depend on multiwavelength analyses of galaxies. CO observations are used to deduce the masses and distributions of molecular hydrogen in galaxies, which are then compared with other tracers (optical and infrared continuum and Hα and H I line radiation). In Section 2, we first discuss CO as a tracer of H_2 mass in spiral galaxies, including new evidence that global H_2 masses for luminous spirals are generally accurate to $\pm 50\%$ (1σ), including both measurement uncertainties and variations galaxy to galaxy in the CO to H_2 conversion constant (Devereux & Young 1990b). We then review the radial distributions of gas and star formation (Section 3), spiral structure (Section 4), molecular properties of galaxies in the Local Group (Section 5), global gas contents (Section 6), star formation rates and efficiencies (Section 7), effects of galactic interactions (Section 8), and nuclear gas concentrations (Section 9).

2. MOLECULAR MASS DETERMINATIONS

Since the H_2 molecule has no permanent electric dipole moment and the lowest quadrupole rotational transitions lie in the infrared, indirect techniques must be utilized to estimate the H_2 abundance in cool, dense clouds. A number of papers have discussed the use of CO as a tracer of the mass of molecular hydrogen (see, for example, Sanders et al 1984, Bloemen et al 1986, Dickman et al 1986, Young et al 1986a, Scoville & Sanders 1987, Maloney & Black 1988, Elmegreen 1989, Devereux & Young 1990b). In spite of the high optical depth of the 2.6 mm CO line, the emission is generally believed to trace the mass of giant molecular clouds (GMCs) in luminous galaxies. In this section, we briefly summarize the theoretical, empirical, and observational basis for the use of CO as a tracer of H_2.

2.1 *Theoretical Basis*

If I_{CO} is the CO brightness temperature integrated over the line profile ($I_{CO} \equiv \int T_{CO}\, dV$), one can define the CO luminosity of a cloud as

$$L_{CO} = D^2 \int I_{CO}\, d\Omega \qquad 1.$$

where D is the distance of the cloud. For a uniform, spherical cloud of radius R, the CO luminosity is given by

$$L_{CO} = \pi R^2 T_{CO} \Delta V \qquad 2.$$

where T_{CO} is the peak brightness temperature in the CO line and ΔV is the linewidth. Numerous studies of Galactic molecular clouds have shown that they are self-gravitating. For a cloud of mass M in virial equilibrium, $\Delta V = \sqrt{GM/R}$ and

$$M_{Cloud} = L_{CO} \sqrt{\frac{4\rho}{3\pi G}} \frac{1}{T_{CO}}. \qquad 3.$$

To the extent that the ratio $\sqrt{\rho}/T_{CO}$ does not vary in the mean from galaxy to galaxy and the emission of separate clouds along each line of sight is not overlapped in velocity, Eq. (3) indicates that the total CO luminosity of a galaxy (summing over all individual clouds in the antenna beam) is directly proportional to the total mass of molecular clouds.

In Galactic GMCs, typical mean densities and CO brightness temperatures are 100–300 H_2 cm^{-3} and 5–10 K (Scoville & Sanders 1987). In the nearby starburst galaxy M82, observations of CO $J = 3 \rightarrow 2$, $2 \rightarrow 1$, and $1 \rightarrow 0$ (Wild et al 1989, Turner et al 1990) indicate the presence of two cloud populations: a cool one ($T \sim 10$–20 K) with low density [$n(H_2) < 10^3$ cm^{-3}], and a warm one ($T \sim 75$ K) with high density [$n(H_2) \sim 5 \times 10^4$ cm^{-3}]. In spite of the markedly different cloud properties in these two components, the difference in $\sqrt{\rho}/T$ between these two populations and the clouds in the Milky Way is only a factor of ~ 1.5. Therefore, even in the extreme conditions encountered in M82, the assumption of a constant conversion factor between CO luminosity and H_2 mass can lead to global molecular gas mass estimates that are reasonably accurate.

Maloney & Black (1988) and Elmegreen (1989) have considered the effects of metallicity variations on the H_2 masses derived from the CO luminosities, and in particular the case of very low metallicity in irregular galaxies in which a reduction in the UV shielding may lead to smaller molecular cores.

2.2 *Empirical Basis*

2.2.1 THE GALAXY A number of observational attempts have been made to determine empirically the constant of proportionality relating H_2 masses to CO luminosities (or equivalently gas column densities to the integrated CO brightness temperature) in Galactic GMCs. The four general techniques that have been applied include (*a*) correlation of CO emission in nearby clouds with the visual extinction (A_V), (*b*) excitation analysis of ^{13}CO and CO emission, (*c*) derivation of virial masses from the CO and ^{13}CO cloud sizes and linewidths, and (*d*) comparison with γ-ray emission. The derived ratios of $N(H_2)/I_{CO}$ range between $1–5 \times 10^{20}$ cm^{-2} [K km s^{-1}]$^{-1}$ (see Table 1 in Scoville & Sanders 1987).

In our opinion, the virial theorem analysis provides the most reliable conversion factor, since it is free of uncertainties in the molecular excitation and the cosmic ray density. Figure 1 shows the correlation between the virial masses of Milky Way molecular clouds and their CO luminosities (Scoville et al 1987, Solomon et al 1987). The virial masses were derived for clouds with known sizes and linewidths, and for clouds with mass between 10^5 and 2×10^6 $M_\odot$, $N(H_2)/I_{CO} \simeq 3.0 \times 10^{20}$ cm^{-2} (K km s^{-1})$^{-1}$, consistent with the γ-ray analysis (2.8×10^{20} cm^{-2} [K km s^{-1}]$^{-1}$) of Bloemen et al (1986). It is noteworthy that no significant large-scale variations in the conversion ratio are seen at radii 2–10 kpc in the inner Galaxy (Bloemen et al 1986, Scoville & Good 1989), and thus variations in metallicity and cloud properties cannot strongly affect the H_2 mass derivations. Throughout this review, we consistently adopt the value of $N(H_2)/I_{CO} = 3.0 \times 10^{20}$ cm^{-2} [K (T_R^*) km s^{-1}]$^{-1}$.

Most of the Galactic data used in the above studies are presented in units of T_R^* (Kutner & Ulich 1981), which does not correct for the coupling between the source and the telescope beam. Since giant molecular clouds have large angular sizes, the coupling efficiency, η_c, is close to unity, and $T_R = T_R^* \eta_C^{-1} \approx T_R^*$. For a galaxy filling only the primary diffraction beam, the coupling efficiency η_c is $\sim$0.8 on several of the telescopes used for extragalactic CO studies and the correction factors appropriate to this case are discussed by Sanders et al (1991). For more extended galaxies, a number of techniques have been used to compute the total CO emission (Stark et al 1986, Solomon & Sage 1988, Verter 1988, Kenney & Young 1988a) and one should be aware of the different assumptions when using these estimates.

2.2.2 EXTERNAL GALAXIES In some of the local group galaxies, several recent investigations have attempted to measure the sizes, linewidths, and CO luminosities of individual molecular clouds to check the applicability

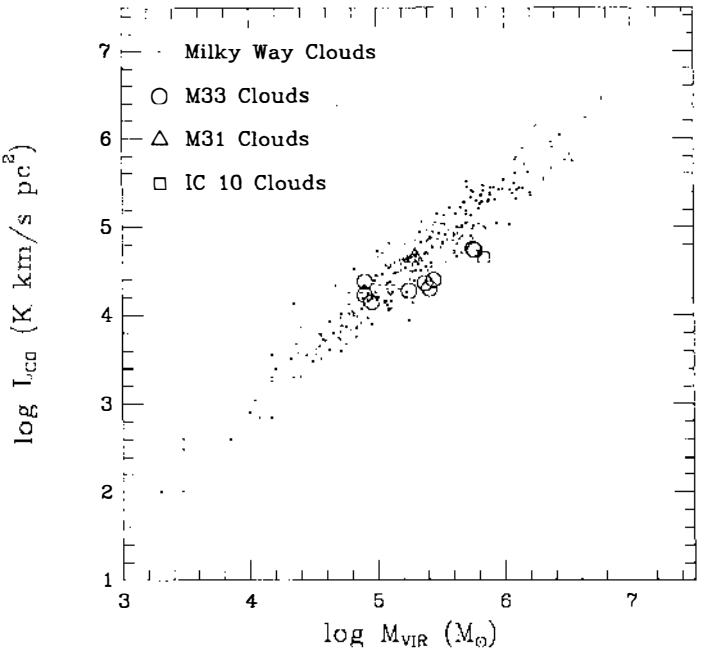

Figure 1 Comparison of CO luminosities and virial masses of molecular clouds in the Milky Way (Scoville et al 1987, Solomon et al 1987), M31 (Vogel et al 1987), M33 (Wilson & Scoville 1990), and in the low-metallicity galaxy IC 10 (Wilson & Reid 1990). In the Milky Way, the CO luminosity is closely correlated with the virial masses of the clouds, both with and without high mass star formation. This linear proportionality justifies the use of CO as a tracer of the mass of H_2; the best fit to these data for clouds with masses between 10^5 and 2×10^6 $M_\odot$ yields a constant of proportionality of 3.0×10^{20} H_2 cm^{-2} (K km s^{-1})$^{-1}$. The similarity of the clouds in M31, M33, and IC 10 to the Milky Way justifies the use of the same CO $\rightarrow$ H_2 proportionality in the external galaxies.

of the Galactic CO to H_2 conversion constant in other environments. In order to measure the sizes of individuals clouds, it is crucial to have a spatial resolution better than 40 pc, the "typical" size of a GMC.

The spiral galaxies M31 and M33 have both been observed with aperture synthesis in CO at 7″ (20 pc) resolution (Vogel et al 1987, Wilson & Scoville 1989, 1990). The CO luminosities and virial masses for the M31, M33, and IC 10 molecular clouds are included in Figure 1 along with the Galactic clouds. The extragalactic molecular clouds are apparently similar to those in the Milky Way, even though they represent regions of lower metallicity (by a factor of 4 relative to the sun; Pagel & Edmunds 1981, Becker 1990,

Wilson & Reid 1991) and are found in galaxies ranging from type Sb (M31) to Scd (M33) to irregular (IC 10).

Moderate resolution studies of the LMC and SMC [8.8′ or 140 pc (Cohen et al 1988)] have also been made. Cohen et al (1988) suggest that the molecular clouds in the LMC have six times more mass per unit CO luminosity than molecular clouds in the Milky Way. It must be borne in mind, however, that their resolution of 140 pc is insufficient to resolve individual molecular clouds similar to Galactic GMCs, and the emission may arise from unbound associations of clouds that are not virialized. Higher angular resolution maps of clouds in the LMC and SMC are essential for establishing the virial masses of individual clouds and to test further the accuracy of H_2 mass determinations in environments with low metallicity.

In addition to ascertaining the absolute accuracy of molecular mass determinations derived using the Galactic CO to H_2 conversion constant, establishing the relative accuracy of H_2 mass determinations from galaxy to galaxy is also important. Devereux & Young (1980b) have compared the inner disk gas masses (molecular plus atomic) with the warm dust masses derived from *IRAS* 60 μm and 100 μm flux densities for 58 luminous spiral galaxies in which the distributions of atomic and molecular gas have been measured. The dispersion of the gas/dust ratio computed from these three independently derived quantities is ± 0.19 dex, a value that is consistent with 30% uncertainties in each of the gas masses and a 10% uncertainty in the warm dust masses. In principle, this 1σ uncertainty of $\pm 30\%$ in global H_2 masses represents both measurement uncertainties and global variations from galaxy to galaxy in the CO $\rightarrow$ H_2 conversion constant. Furthermore, Devereux & Young (1990b) point out that the similar scatter for the H I and H_2 dominated galaxies (see Figure 6b) indicates that global molecular gas masses in galaxies are apparently as accurately determined as the atomic gas masses for luminous spirals.

3. RADIAL DISTRIBUTIONS IN SPIRAL GALAXIES

The radial distributions of molecular gas have been measured in over 100 galaxies (see Table 1). In this section, we review *azimuthally averaged* CO radial distributions in galaxies as a function of morphological type. This discussion refers to observations at 45–60″ resolution, typically 1 to 4 kpc.

3.1 *Unbarred Spiral Galaxies*

There are 40 Sc galaxies whose CO radial distributions have been measured along the major axis. Figure 2a shows the CO integrated intensity dis-

Table 1 CO studies in individual galaxies

Galaxy	Type[a]	Telescope[b]	Resolution (arcsec)	Reference
NGC 55	Sc	SEST	44	Dettmar & Heithausen (1989)
NGC 224 (M31)	SbI-II	BTL	100	Stark (1979)
		OSO	33	Boulanger et al (1984)
		BTL	100	Ryden and Stark (1986)
		NRO	15	Ichikawa et al (1987)
		NRO	15	Lada et al (1988)
		OVRO	7	Vogel et al (1987)
		IRAM	23	Casoli & Combes (1988)
		OSO	33	Sandquist et al (1990)
NGC 253	Sc(s)	NRAO	67	Rickard et al (1977)
		FCRAO	45	Scoville et al (1985)
		OVRO	7	Canzian et al (1988)
NGC 404	S0	IRAM	14, 22	Wiklind & Henkel (1990)
NGC 520	Merger	OVRO	5	Sanders et al (1988a)
NGC 598 (M33)	Sc(s)II-III	FCRAO	45	Young & Scoville (1982c)
		NRAO	60	Wilson & Scoville (1989)
		OVRO	6	Wilson & Scoville (1990)
NGC 891	Sb on edge	FCRAO	45	Solomon (1982)
		NRO	15	Sofue et al (1987)
		FCRAO	45	Young (1987)
NGC 1068	Sb(rs)II	FCRAO	45	Scoville et al (1983)
		OVRO	7	Myers & Scoville (1987)
		IRAM	21	Planesas et al (1989)
		NRO	15	Kaneko et al (1989)
		OVRO	3	Planesas et al (1991)
NGC 1097	RSBbc(rs)I-II	IRAM	21	Gerin et al (1988)
NGC 1275	E pec	IRAM	21	Lazareff et al (1989)
NGC 1365	SBb(s)I	OSO	33	Sandquist et al (1988)
NGC 1569	SmIV	FCRAO	45	Young et al (1984a)
		NRAO	60	Hunter et al (1989)
NGC 2146	SbII pec	FCRAO	45	Young et al (1986a)
		BIMA	7	Jackson & Ho (1988)
		OVRO	7	Young et al (1988b)
NGC 2403	Sc(s)III	FCRAO	45	Young & Scoville (1982c)
NGC 2623	Merger	IRAM	12	Casoli et al (1988)
NGC 2685	Polar Ring	NRO	15	Taniguchi et al (1990)
NGC 2841	Sb	FCRAO	45	Young & Scoville (1982b)
NGC 3031 (M81)	Sb	NRAO	60	Combes & Gerin (1985)
		IRAM	22	Brouillet et al (1990)
NGC 3034 (M82)	Amorphous	NRAO	67	Rickard et al (1977)
		FCRAO	45	Young & Scoville (1984)
		OSO	33	Olofsson & Rydbeck (1984)
		NRO	15	Nakai et al (1987)
		OVRO	7	Lo et al (1987b)
		BIMA	7	Carlstrom (1988)
		IRAM	13	Loiseau et al (1988)
		IRAM	9, 12	Wild et al (1989)
		NRAO	30	Philips & Mampaso (1989)
		NRAO	22	Turner et al (1990)
		JCMT	13	Tilanus et al (1991)
NGC 3077	Amorphous	IRAM	14, 22	Becker et al (1989)
NGC 3079	Sc pec	FCRAO	45	Young et al (1986a)
		OVRO	7	Young et al (1988a)
NGC 3147	Sb(s)I.8	FCRAO	45	Young et al (1986a)
NGC 3227	Sb	BIMA	3	Meixner et al (1990)
NGC 3256	Irr	CSO	30	Sargent et al (1989)

Table 1 *continued.*

Galaxy	Type[a]	Telescope[b]	Resolution (arcsec)	Reference
NGC 3351	SBb	OVRO, FCRAO	7, 45	Devereux et al (1991)
NGC 3593	Sa pec	NRAO	60	Hunter et al (1989)
NGC 3623	Sa(s)II	FCRAO	45	Young et al (1983)
NGC 3267	Sb(s)II.2	FCRAO	45	Young et al (1983)
NGC 3628	Sbc	FCRAO	45	Young et al (1983)
NGC 3738	SdIII	FCRAO	45	Tacconi & Young (1985)
NGC 4038/39	pair	OVRO	6	Stanford et al (1990)
NGC 4214	I	NRAO	60	Thronson et al (1988)
NGC 4258	Sb(s)II	NRO	15	Sofue et al (1989a)
		IRAM	22	Krause et al (1990)
NGC 4418	S0/Sa	NRO	15	Kawara et al (1990)
NGC 4419	SBab	FCRAO	45	Kenney et al (1990)
Virgo Cluster	52 Spirals	FCRAO	45	Kenney & Young (1986, 1988a,b, 1989)
	47 Spirals	BTL	100	Stark et al (1986)
	8 Spirals	OVRO	6	Canzian (1990)
NGC 4438	Sb (tides)	IRAM	21	Combes et al (1988)
NGC 4449	SmIV	FCRAO	45	Tacconi & Young (1985)
		NRAO	60	Thronson et al (1987)
		NRO	15	Sasaki et al (1990)
NGC 4472	E	IRAM	21	Huchtmeier et al (1988)
NGC 4485/90	Pair	NRAO	60	Thronson et al (1989a)
NGC 4565	Sb	BTL	100	Richmond & Knapp (1986)
NGC 4631	Sc	NRO	15	Sofue et al (1989b)
NGC 4736	RSab(s)	FCRAO	45	Garman & Young (1986)
NGC 4945	Irr	SEST	43	Whiteoak et al (1990)
NGC 5005	Sb(s)II	FCRAO	45	Young et al (1986a)
NGC 5055	Sbc(s)II-III	OSO	33	Johansson & Booth (1987)
NGC 5128 (Cen A)	SO pec	CSO	30	Phillips et al (1987)
		SEST	40	Israel et al (1990)
NGC 5194	Sbc(s)I-II	NRAO	67	Rickard & Palmer (1981)
		FCRAO	45	Scoville & Young (1983)
		OSO	33	Rydbeck et al (1985)
		OVRO	7	Lo et al (1987a)
		OVRO	7	Vogel et al (1988)
		IRAM	12	Guelin et al (1988)
		IRAM	12	Garcia-Byrillo & Guelin (1990)
		OVRO	7	Rand & Kulkarni (1990)
		FCRAO	45	Lord & Young (1990)
NGC 5195	SBO pec	FCRAO	45	Lord & Young (1990)
		NRAO	60	Sage (1989)
NGC 5236 (M83)	SBc(s)II)	NRAO	67	Combes et al (1978)
		FCRAO	45	Lord (1987)
		NRO	15	Handa et al (1990)
		OVRO	6	Kenney & Lord (1991)
		SEST	43, 23	Wiklind et al (1990)
NGC 5383		NRO	15	Ohta et al (1986)
NGC 5457 (M101)	Sc(s)I	NRAO	67	Solomon et al (1983)
		NRAO	60	Kenney et al (1991)
NGC 6946	Sc(s)II	NRAO	67	Morris & Lo (1978)
		NRAO	67	Rickard & Palmer (1981)
		FCRAO	45	Young & Scoville (1982a)
		OVRO	7	Ball et al (1985)

Table 1 *continued.*

Galaxy	Type[a]	Telescope[b]	Resolution (arcsec)	Reference
NGC 6946		FCRAO	45	Tacconi & Young (1986, 1989)
		IRAM	21	Weliachew et al (1988)
		NRO	15	Sofue et al (1988)
		IRAM	14, 23	Casoli et al (1990)
		NMA	7	Ishizuki et al (1990b)
NGC 7331	Sb(rs)I-II	FCRAO	45	Young & Scoville (1982b)
NGC 7469	Sab pec	NRAO	60	Heckman et al (1986)
		OVRO	5	Sanders et al (1989)
		BIMA	3	Meixner et al (1990)
NGC 7479	SBbc(s)I-II	FCRAO	45	Young et al (1986a)
Arp 55	Irr	OVRO	5	Sanders et al (1988a)
Arp 220	Merger	IRAM	12	Casoli et al (1988)
		OVRO	5	Scoville et al (1986b)
		IRAM	21	Solomon et al (1990)
		OVRO	2	Scoville et al (1991)
IC 10	Im	NRO	15	Ohta et al (1988)
		IRAM	12	Becker (1990)
		OVRO	7	Wilson & Reid (1990)
IC 342	SAB(rs)cd	NRAO	67	Morris & Lo (1978)
		NRAO	67	Rickard & Palmer (1981)
		FCRAO	45	Young & Scoville (1982a)
		OVRO	7	Lo et al (1984)
		NRAO	20	Ho et al (1987)
		OSO	33	Wilkind et al (1987)
		NRO	15	Hayashi et al (1987)
		IRAM	8	Maurersberger et al (1990)
		CSO	24	Wall & Jaffe (1990)
		NRO	3	Ishizuki et al (1990a)
IC 694/NGC 3690	pair	OVRO	5	Sargent et al (1987)
		IRAM	12, 21	Casoli et al (1989)
		OVRO	2	Sargent & Scoville (1991)
Maffei II	Sb	NRAO	67	Rickard et al (1977)
		IRAM	21	Weliachew et al (1988)
		NRO	5	Ishiguro et al (1989)
		OVRO	7	Hurt & Turner (1991)
Mrk 231	Seyfert/QSO	FCRAO	45	Sanders et al (1987)
		OVRO	7	Scoville et al (1989)
Mrk 297	Irr	NRO	15	Sofue et al (1990)
Mrk 1014	Quasar	NRAO	60	Sanders et al (1988b)
VII Zw 31		FCRAO	45	Sage & Solomon (1987)
		OVRO	5	Scoville et al (1989)
I Zw 1	Quasar	IRAM	21	Barvainis et al (1989)
IRAS 12112+0305		NRAO	67	Mirabel et al (1988a)
LMC and SMC	SB(s)m		120	Israel et al (1986)
			530	Cohen et al (1988)
			530	Rubio et al (1991)

[a] Galaxy type from *Revised Shapley Ames Catalogue* (Sandage & Tammann 1981, hereafter RSA).

[b] Key for telescopes: BIMA = Berkeley Illinois Maryland Array, BTL = Bell Telephone Laboratories, CSO = Caltech Submillimeter Observatory, FCRAO = Five College Radio Astronomy Observatory, IRAM = Inst. Radio Astronomie Millimetrique, JCMT = James Clark Maxwell Telescope, NRAO = National Radio Astronomy Observatory, NRO = Nobeyama Radio Observatory, OSO = Onsala Space Observatory, OVRO = Owens Valley Radio Observatory.

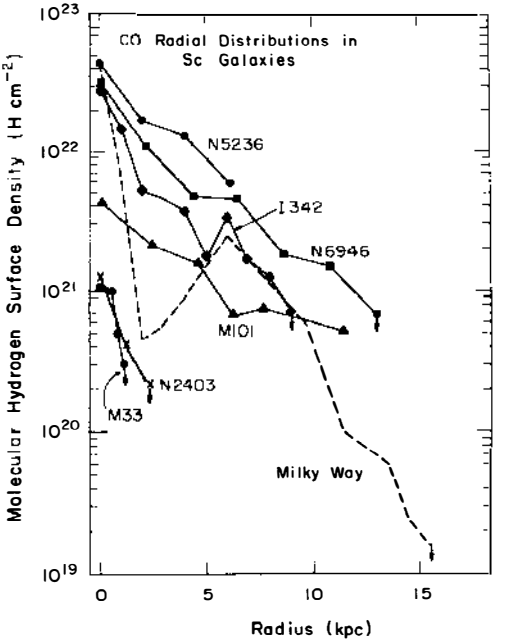

Figure 2a Radial distributions of CO integrated intensity, corrected to face-on, for six relatively face-on Sc galaxies (*solid lines*) and the Milky Way (*dashed line*, Sanders et al 1984). Galaxy types and references for the CO distributions are found in Table 2 and distances are given in Young et al (1989).

tributions for a sample of Sc galaxies, with the observed intensities corrected for inclination (as described in Young & Scoville 1982a). Also shown in Figure 2a is the Milky Way CO distribution smoothed to 1 kpc resolution (Sanders et al 1984), illustrating the central peak, the absence of gas between 1 and 4 kpc, and the molecular annulus between 4 and 8 kpc. None of the face-on Sc galaxies has CO radial distributions that resemble that in the Milky Way. The dominant characteristic of the CO distributions for the Sc galaxies is a central peak and monotonic intensity falloff with increasing radius. For a given galaxy, there is typically a factor of 2 variation in the CO integrated intensities at different azimuthal angles, relative to the mean value at each radius (Morris & Rickard 1982, Young & Scoville 1982a, Solomon et al 1983, Scoville & Young 1983, Tacconi & Young 1986, 1990, Kenney & Young 1988a, Lord & Young 1990, Kenney et al 1991).

In luminous, face-on, late-type spirals, the azimuthally averaged distributions of H_2 are markedly different from those of H I in the same

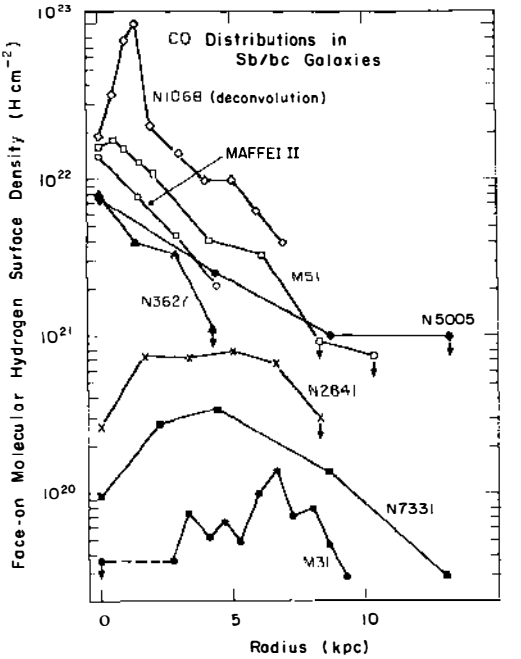

Figure 2b Radial distributions of CO integrated intensity, corrected to face-on, for eight Sb/Sbc galaxies. Galaxy types and references for the CO distributions are found in Table 2. The CO distribution for M31 has been scaled down by a factor of 5. Five of these galaxies exhibit central CO depressions.

galaxies (Morris & Rickard 1982, Young & Scoville 1982a, Scoville & Young 1983, Kenney & Young 1989). The central peaks in the H_2 distributions for Sc galaxies contrast markedly with the central depressions seen in H I and the relatively constant H I surface densities [$N(\text{H I}) \leq 10^{21}$ cm^{-2}] across the optical disk, outside the center. In NGC 6946 (see Section 7.1), the ratio of H_2 to H I surface densities decreases from a central value of 30 to unity at a radius of 10 kpc (Tacconi & Young 1986). In most of the luminous Sc galaxies, the molecular gas more than fills in the central hole present in the atomic gas distributions.

The total number of Sb and Sbc galaxies in which the CO distributions have been measured is 25. Among the Sb galaxies that are at distances of less than 25 Mpc (for $H_0 = 50$ km s^{-1} Mpc^{-1}), fewer than half have been found to exhibit CO depressions in their centers. These galaxies include M31 (Stark 1979), NGC 2841 and 7331 (Young & Scoville 1982b), NGC 1068 (Scoville et al 1983, Myers & Scoville 1987), NGC 891 (Sofue 1988,

Young 1987), NGC 4216 (Kenney & Young 1988a), and NGC 488, 2336, 3147, 4725, and IC 356 (Young et al 1991). Figure 2b illustrates the CO radial distributions for a sample of Sb galaxies with and without central CO depressions. There is no obvious correlation of the presence or absence of the central CO depression with other galaxy properties.

Major axis CO distributions in early type spiral galaxies have been published for only a small number of systems, most of which exhibit CO radial distributions that peak in the center and decrease monotonically with radius, like the Sc galaxies and the majority of the Sb galaxies. The central H_2 surface densities in the early type galaxies are as high as those found in the Sc galaxies. The H I distributions for Sa galaxies, on the other hand, have surface densities that peak at 1–4 $M_\odot$ pc^{-2}, as opposed to 5–10 $M_\odot$ pc^{-2} found for Sc galaxies (Wevers et al 1986, van Driel 1987).

The isophotal diameters for the CO emission in a large sample of spiral galaxies have been analyzed by Kenney & Young (1988a). Overall, the mean ratio of CO diameter to optical diameter (D_{25}) for 68 galaxies has a value of 0.5 ± 0.2, with a tendency for the largest ratios to be found in the late type spirals.

3.2 *Barred Spiral Galaxies*

Optically barred spiral galaxies in which the distribution of molecular matter has been mapped include NGC 5236 (M83) (Combes et al 1978, Lord 1987), NGC 1097 (Gerin et al 1988), and NGC 1365 (Sandquist et al 1988). In all cases, the CO emission is clearly enhanced along the bar. High resolution mapping of CO in NGC 253 has also shown the molecular gas strongly concentrated along the central bar seen in the near infrared (Canzian et al 1988). In the barred spiral galaxy NGC 3351, a nuclear molecular gas bar is found perpendicular to the optical bar (Devereux et al 1991). Several galaxies that do not show obvious barred morphology in the optical have been found to exhibit elongated CO distributions in their centers. High resolution CO observations of IC 342 and NGC 6946 indicate that both of these galaxies have a CO bar in the central arcminute (Lo et al 1984, Ball et al 1985). In IC 342, the CO has been resolved into two offset ridges along the leading edges of the rotating bar (Ishizuki et al 1990). These studies support the theoretical prediction that the bar may promote the inward transfer of gas to the center of the galaxy, thus fueling a central burst of star formation (Sanders & Huntley 1976, Roberts et al 1979).

3.3 *^{13}CO Observations of Galaxies*

A second test of the molecular mass determinations is comparison of the CO radial distribution in a galaxy with that of the more optically thin

^{13}CO line. The first ^{13}CO observations in eight galaxies (Encrenaz et al 1979) were followed by additional studies in a small number of other systems (Young & Scoville 1982a, 1984, Stark & Carlson 1984, Rydbeck et al 1985). Defining the ratio of CO to ^{13}CO integrated intensities to be $R \equiv I(\mathrm{CO})/I(^{13}\mathrm{CO})$, Encrenaz et al (1979) found an average value of $R \sim 12$, or roughly twice the mean value in the molecular annulus of our Galaxy (Solomon et al 1979, Stark 1983). Rickard & Blitz (1985) and Young & Sanders (1986) measured the CO and ^{13}CO emission in the disks of several nearby luminous spiral galaxies. In six galaxies, the shapes of the azimuthally averaged distributions for CO and ^{13}CO were similar. Globally, the value of R was found to range between 6 and 20 for individual galaxies, with the lower values in NGC 891. The highest value of R was found in the center of M82, where the ratio of integrated intensities was 20. Within individual galaxies, R varied by a factor of 2 on the scale of 1 to 2 kpc. Such variations could be caused by changes in the relative percentage of hot and cold clouds, such as is seen in the Milky Way between spiral arm and interarm regions (Solomon et al 1985).

4. SPIRAL STRUCTURE IN M51

Ever since the earliest observations of molecular clouds in galaxies, there has been great interest in determining the extent to which the molecular clouds and their properties are correlated with spiral arms. Density waves, believed to be responsible for the spiral pattern in some galaxies, might provide a mechanism for molecular *cloud growth* either through gravitational instabilities or by increasing the incidence of cloud-cloud collisions and coalescence. Numerous studies have shown, however, that the molecular gas is widespread and not confined solely to the spiral arms. Although the early CO observations employing 45 to 66″ beams (Rickard & Palmer 1981, Young & Scoville 1982a, Scoville & Young 1983) had resolution only marginally sufficient to separate the arm and interarm regions, recent higher resolution studies have confirmed that although significant spiral arm concentrations do exist, most of the molecular emission originates from interarm regions.

Perhaps the best example of a galaxy in which to investigate the extent to which the molecules are confined to spiral arms is M51. In this grand design spiral, the exceptionally strong arms probably result from both density waves (in the inner disk) and the tidal interaction with NGC 5195 (in the outer disk). At 33″ resolution, i.e. 1.6 kpc, the CO enhancement is 20% in the arms and the underlying axisymmetric, exponential disk contributes ~75% of the total emission (Rydbeck et al 1985).

Aperture synthesis mapping of the CO in M51 at 7″ resolution has been

reported by Lo et al (1987a), Vogel et al (1988), and Rand & Kulkarni (1990). The interferometric data (see Figure 3) show striking concentrations of CO emission along the dust arms, displaced on average by approximately 7″ (300 pc) to the inside (upstream direction) of the arms seen in Hα. The masses of these molecular cloud associations are 10^7–6×10^7 $M_\odot$. The CO emission maxima coincide precisely with regions of enhanced dust obscuration in optical continuum images. Approximately 25% of the total CO emission is contained in the arm-like structures shown in Figure 3, with an arm-interarm contrast of approximately 3:1 averaged over scales of 500 pc (Vogel et al 1988, Guelin et al 1988). Discrete emission concentrations are also seen in the areas between the arms, although they are not so well organized into coherent structures (Rand & Kulkarni 1990). It is noteworthy that the spiral arms seen in nonthermal radio continuum are aligned most closely with the CO ridges shown in Figure 3, whereas the 21 cm H I emission concentrations are displaced downstream near the Hα arms (Rand & Tilanus 1990). Presumably, this H I arises from dissociation of molecular gas by young stars formed in the arms. Even in the downstream areas, the single dish data indicate that the surface density of molecular gas still exceeds that of atomic gas. Thus, the molecular gas is not significantly dissociated by the OB star formation, but is instead distributed into smaller structures (e.g. individual GMCs) that are less easily detected by the interferometer.

The CO studies in M51 suggest a picture in which pre-existing GMCs come into the arm from the back side, concentrate in large cloud complexes as a result of orbit crowding or gravitational instabilities in the potential well of the spiral arm, and form high mass stars slightly downstream of the potential minimum. The OB stars then dissociate some of the molecular gas to produce the Hα and H I ridges downstream from the molecular peak. The disappearance of the molecular cloud *complexes* on the downstream side of the spiral arms could result from expected divergence of the cloud orbits as they come out of the spiral potential or the disruptive effects of high mass star formation. Inasmuch as the quantity of atomic and ionized gas in the downstream direction is significantly less than the abundance of molecular gas at the spiral ridge, the former may be the primary cause.

The extent to which the M51 results may be applied to other spiral galaxies, in particular to those with lower gas densities or those with smaller spiral arm amplitudes, is not at all clear. All of the processes discussed above (orbit crowding, gravitational instability, and cloud disruption as a result of OB star formation) are likely to be most significant in a galaxy like M51 with a strong spiral pattern, a high interstellar gas density, and a high rate of OB star formation. Significant downstream

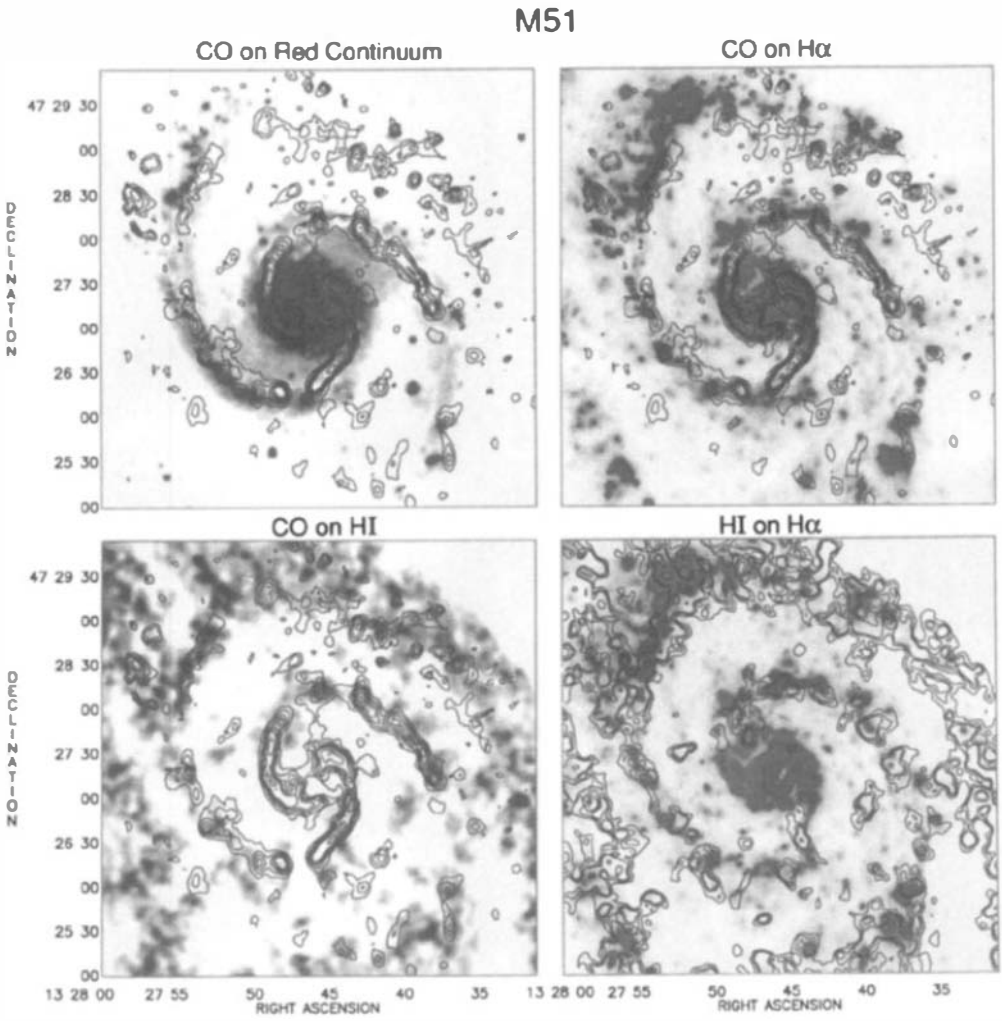

Figure 3 Mosaic map of the CO emission at 7″ (350 pc) resolution in M51 superposed on gray scale images of the red continuum (*upper left*), Hα (*upper right*), and 21 cm H I emission (*lower left*) (Rand & Kulkarni 1990). On the lower right, the H I emission contours (Rots et al 1990) are superposed on a gray scale image of Hα. The spiral arm concentrations of CO emission are closely aligned with areas of increased dust obscuration seen in the red continuum images (*upper left*), but displaced approximately 300 pc upstream of the spiral arm H II regions (*upper right*) and H I gas (*lower left*). The CO interferometry recovers approximately 30% of the total CO line flux; the remaining molecular emission is more uniformly distributed on scales $\lesssim 25''$.

offsets of the H I spiral arms from the dust lanes have been noted by Allen et al (1986) for the barred spiral galaxy M83; on the other hand, Lada et al (1988) found a close correlation between the atomic and molecular ridges in M31 in both velocity and space (see Section 5.1). We therefore caution that the results in either M51 or M31 should not be taken as a general rule; instead, these two situations may represent gas-rich and gas-poor galaxies, respectively.

5. LOCAL GROUP GALAXIES

M31 and M33 are prime galaxies in which to study the detailed distribution of molecular clouds, due to their proximity ($\sim$700 kpc). Because they cover such large areas on the sky, most studies have concentrated on selected regions, either to determine the CO radial distributions, to correlate CO emission with the spiral arms, or to investigate individual GMCs.

The first investigation of the CO in M31 consisted of observations at 90″ resolution along the minor axis (Stark 1979), revealing an absence of molecular clouds in the central region and an annulus of emission coincident with the optical arms. Along the minor axis, the inferred H_2 surface density is less than or equal to that of H I at all radii (Brinks 1985). Numerous investigations of the concentration of molecular clouds in spiral arms have been conducted for M31 (Combes et al 1977a,b, Boulanger et al 1984, Ryden & Stark 1986, Lada et al 1988). Ryden & Stark (1986) found an arm-interarm contrast of 7 ± 4 and kinematic evidence of streaming across the spiral arms.

In a recent CO study, in which individual GMCs in M31 were partially resolved, Lada et al (1988) inferred sizes, densities, and masses similar to those of GMCs in the solar neighborhood. Comparison with H I observations led them to conclude that the GMC-H I complexes have total gas (H_2 + H I) masses on the order of 10^6 $M_\odot$, of which $\sim$30% is atomic. They infer that the gas column density threshold for H_2 formation is similar to that estimated for clouds in the Milky Way.

CO emission in the nuclear region of M33 has been observed with both single dish and aperture synthesis out to 3.5′ (1 kpc) radius by Wilson & Scoville (1989, 1990). The single dish map shows emission complexes with sizes 200–400 pc and masses 3–10 $\times$ 10^6 $M_\odot$ some of which are associated with the two spiral arms in this area of the galaxy. The structures are neither tidally nor virially bound and must therefore be transient associations of smaller clouds. The interferometric measurements do reveal individual GMC-type clouds with masses and CO luminosities consistent with their being self-gravitating (see Section 2.2.2).

The Large and Small Magellanic Clouds are sufficiently nearby that they provide the opportunity of achieving high spatial resolution (1′ = 23 pc) relative to the sizes of the molecular clouds within them. The most comprehensive study is that of Cohen et al (1988), who obtained a fully sampled CO map at 8.8′ resolution (200 pc) of the central 6° × 6° in the LMC and detected CO emission in approximately 10% of the region studied. They found that emission is dominated by a molecular cloud complex extending several kpc south of 30 Doradus. High velocity CO emission was also seen in this region, possibly arising from gas accelerated by stellar winds and supernovae. An extensive high resolution CO survey of the LMC is currently in progress with the SEST telescope.

6. GLOBAL H_2, H I, AND IR IN GALAXIES

A major goal of extragalactic CO studies has been to understand the evolution of galaxies through comparison of the gas contents (H_2 and H I) and star formation rates as a function of galaxy type, luminosity, and environment. Initial studies in this area were conducted by the investigators listed in Table 2, with statistical analyses presented by Rengarajan & Verma (1986), Verter (1987), and Young et al (1989). Here, we consider the global properties of over 300 galaxies from numerous studies (see Table 2), in which CO was mapped to determine the global flux.

6.1 *Total H_2 Masses*

The masses of molecular gas that are derived for galaxies cover a broad range, from 5×10^{10} $M_\odot$ for the most massive (Solomon & Sage 1988, Young et al 1989, Sanders et al 1991) to less than 10^6 $M_\odot$ for some low-mass dwarfs (Tacconi & Young 1987), adopting the same CO → H_2 conversion constant as for the massive spirals. The range of H I masses found in the same galaxies is similar (Young et al 1989).

6.2 *Ratio of H_2 to H I*

In order to elucidate the processes that influence molecular cloud formation, it is helpful to analyze the relative amounts of atomic and molecular gas. That there is a morphological type dependence to the (normalized) total atomic gas content of galaxies has long been recognized. In particular, Roberts (1969) showed that the H I mass-to-blue-luminosity ratio, $M(\mathrm{H\,I})/L_B$, increase by a factor of ~ 5 among spiral galaxies going from type Sa to Scd. (This trend is partially due to the contribution of the bulge to the blue luminosity in early type galaxies.)

Young & Knezek (1989) analyzed the global ratios of H_2 to H I for 170

Table 2 Published surveys of CO in galaxies

Galaxy Class	Sample Size	No. Detected	Telescope[a]	Reference
Ellipticals	1	1	IRAM	Huchtmeier et al (1988)
	7	2	IRAM	Gordon (1991)
IR Bright				
Centers	20	10	FCRAO	Young et al (1984b)
Maps	14	14	FCRAO	Young et al (1986a)
High Luminosity	15	15	FCRAO	Sanders et al (1986)
High Luminosity	3	3	OVRO	Sanders et al (1988a)
Ultra-high Lum.	5	4	SEST	Mirabel et al (1988b)
High Luminosity	4	4	OVRO	Scoville et al (1989)
Global Properties	124	108	FCRAO	Young et al (1989)
Maps	29	29	NRAO	Tinney et al (1990)
High Luminosity	60	60	NRAO	Sanders et al (1991)
Irregulars				
Magellanic	6	1	NRAO	Elmegreen et al (1980)
Star-forming	1	1	FCRAO	Young et al (1984a)
Star-forming	3	3	FCRAO	Tacconi & Young (1985)
Clumpy Irregulars	2	0	NRO	Sofue et al (1986)
Dwarf Irr's	15	6	FCRAO	Tacconi & Young (1987)
Blue Compact Galaxies	12	0	IRAM	Arnault et al (1988)
Isolated and Interacting				
Maps	26	26	FCRAO	Young et al (1986b)
Maps	93	90	FCRAO/NRAO	Solomon & Sage (1988)
Markarian	14	14	IRAM	Krugel et al (1990)
Quasars	1	1	IRAM	Barvainis et al (1989)
	1	1	IRAM	Sanders et al (1989)
Radio Bright	21	20	FCRAO/NRAO	Sanders & Mirabel (1985)
Seyferts	9	2	NRAO/BTL	Bieging et al (1981)
	9	0	NRAO	Wilson et al (1979)
	43	18	NRAO	Heckman et al (1989)
	2	2	IRAM	Sanders et al (1989)
	3	2	BIMA	Meixner et al (1990)
	12	4	NRO	Taniguchi et al (1990a)
S0s				
Centers	11	5	NRAO	Sage and Wrobel (1989)
S0-Sa	20	11	FCRAO	Thronson et al (1989a)
E-S0	24	22	OSO, SEST, IRAM	Wiklind & Henkel (1989)
Spirals				
Gas-rich	29	5	NRAO	Rickard et al (1977)
Nearby	81	5	NRAO	Rowan-Robinson et al (1980)
Range of				
Arm Types	29	20	BTL	Stark et al (1987)
Hubble Types	19	6	BTL	Verter (1983)
SAB Galaxies	23	5	NRAO	Elmegreen & Elmegreen (1982)
Sc's	9	9	FCRAO	Young & Scoville (1982b)
Spirals	13	11	NRAO	Adler & Liszt (1989)
Starbursts	42	9	FCRAO	Jackson et al (1989)
Nuclear Starburts	18	16	FCRAO	Young & Devereux (1991)
Virgo Cluster				
Centers	25	18	FCRAO	Young et al (1985)
Centers	7	7	OVRO	Canzian (1990)
Major Axis Maps	52	34	FCRAO	Kenney & Young (1986, 1988a, b, 1989)
Total CO	47	25	BTL	Stark et al (1986)
^{13}CO Observations				
Centers	8	5	BTL	Encrenaz et al (1979)
Disks	6	6	NRAO	Rickard & Blitz (1985)
Disks	6	6	FCRAO	Young & Sanders (1986)

[a] Telescopes are as in Table 1.

galaxies for which H I masses were available in the literature (Huchtmeier et al 1983). Within this sample, the mean ratio of total H I mass to blue luminosity increases with type by a factor of 5, but the mean ratio of H_2 mass to blue luminosity is roughly the same for types Sa–Sc, then decreasing by a factor of at least 3 for types Scd–Sdm. The $M(H_2)/M(HI)$ ratio is shown in Figure 4 for the galaxies in several studies (Young & Knezek 1989, Thronson et al 1989b). While there is considerable scatter in the ratio of H_2 to H I within a given type, the mean clearly changes systematically along the Hubble sequence. A volume limited sample of galaxies closer than 20 Mpc displays a similar decrease in the H_2/H I ratio. Thus, the ratio of molecular to atomic mass decreases by more than a factor of 10 as a function of morphological type for types Sa–Sd. The mean $M(H_2)/M(HI)$ ratio is 4.0 ± 1.9 for SO/Sa galaxies, and 0.2 ± 0.1 for Sd/Sm galaxies. Verter (1987) reached a somewhat different conclusion—that the CO/H I flux ratio peaks for intermediate morphological types—but her study was based on many fewer galaxies.

The *mean* ratio of total ISM mass ($HI + H_2$) to optical area is $17\ M_\odot\ pc^{-2}$, with only a factor of 2 increases from early to late type spirals. Thus, late type galaxies have only marginally greater gas surface densities than the early type galaxies, but the phase of the gas for the cool ISM varies quite systematically along the Hubble sequence. In particular, the late type spiral galaxies have a lower global molecular gas fraction.

Variations in the H_2/H I ratio can result from changes in the efficiency of H_2 cloud formation or the rate of cloud disruption (Wyse 1986, Tacconi & Young 1986, Shaya & Federman 1987, Wyse & Silk 1989, Wang 1990). The variation with morphological type could indicate that the efficiency of molecular cloud formation is higher in early- than in late-type spirals, thus suggesting that large-scale gravitational effects may influence molecular cloud formation.

Recent observations of molecular and atomic gas in infrared bright galaxies indicate that the ISM in interacting systems may be predominately molecular (Mirabel & Sanders 1989, Knezek & Young 1989). Such a situation could arise through enhanced conversion of atomic to molecular gas during interactions, through removal of the loosely bound atomic gas, or both.

It is well known that the atomic gas content of many Virgo spirals is low by factors ranging from 2 to 10, compared with more isolated galaxies of the same type and optical size (Giovanelli & Haynes 1983, van Gorkom & Kotanyi 1985, Warmels 1986), and this depletion has been commonly interpreted as evidence of gas stripping in the cluster environment. Several surveys of CO emission have been conducted for the Virgo spiral galaxies (Kenney & Young 1986, 1989, Stark et al 1986). These studies show that

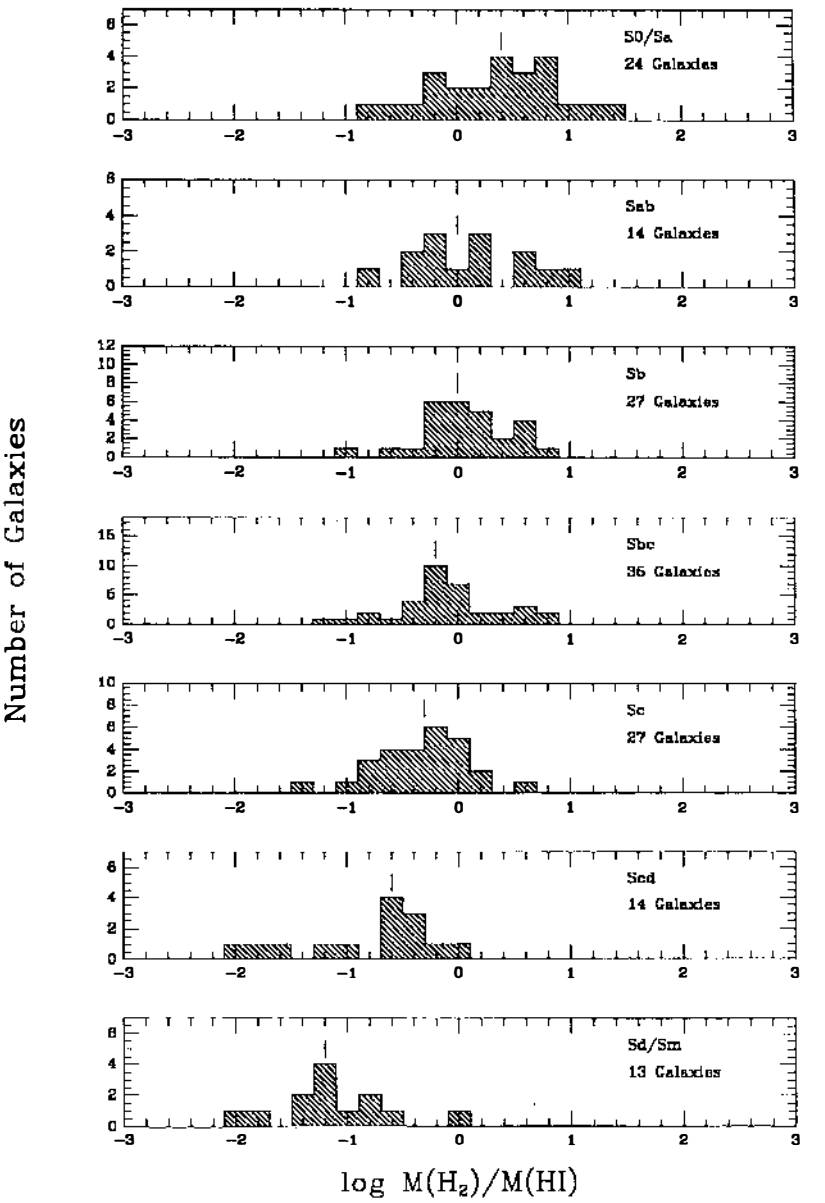

Figure 4 Ratio of molecular to atomic gas mass as a function of morphological type for spiral galaxies (Young & Knezek 1989, Thronson et al 1989). The *vertical tick mark* in each panel represents the median value for that type. Although there is a considerable range in the H_2/HI ratio within each type, the mean value clearly decreases for later type spirals.

the H_2 is not deficient, that is, the mechanism removing the low density atomic gas has left the denser molecular clouds intact. Since the greatest H I depletion in the Virgo spirals occurs in the outer disks, well outside of the region in which most of the molecular gas is usually located in spiral galaxies, it is not suprising that the molecular gas does not show the same degree of depletion as the atomic gas. In addition, the molecular clouds have high column densities and, residing in the inner galaxy, are more tightly bound. The depletion of the H I in the outer disks of some Virgo spirals is approximately a factor of 10, whereas in the inner disk, it is usually a factor of 2 or less (Kenney & Young 1989). Thus, a possible interpretation of the H I and CO data for the Virgo spirals is that the gas depletion occurs entirely in the areas of the galaxy in which the gas is both tenuous and loosely bound by gravitation (i.e. the outer disk or at moderate z above or below the galactic plane).

6.3 *Gas Mass Fractions in Spiral Galaxies*

Using the dynamical mass-to-light ratios of Rubin et al (1985)—in which the ratio M_{dyn}/L_B is $6.2\,M_\odot L_\odot^{-1}$ for Sa galaxies, $4.5\,M_\odot L_\odot^{-1}$ for Sb galaxies, and $2.6\,M_\odot L_\odot^{-1}$ for Sc galaxies—in conjunction with the blue luminosities from RC2, Young & Knezek (1989) computed the dynamical masses of spiral galaxies for which H_2 and H I masses are known. The mean ratio of total neutral gas mass [H I + H_2] to dynamical mass, M_{gas}/M_{dyn}, ranges from 4% for Sa galaxies to 25% for Scd galaxies, as shown in Figure 5. The early type galaxies have thus locked up a much larger fraction of their mass in stars than late type galaxies. It is rather remarkable, then, that the present mean gas surface densities in early type spiral galaxies are only a factor of two lower than in late types (see Section 6.2).

6.4 *The Gas-to-Dust Ratio in Spiral Galaxies*

Comparison of molecular gas masses with *IRAS*-derived dust masses leads to mean gas-to-dust mass ratios of $\sim$600 (Young et al 1986a, 1989, Stark et al 1986, Devereux & Young 1990b, Sanders et al 1991), rather than the value of $\sim$150, which is widely used for the Galaxy (Spitzer 1978, Hildebrand 1983, Draine & Lee 1984). The inclusion of atomic gas in spiral galaxies only accentuates the discrepancy. A plausible explanation for the high apparent gas-to-dust ratio is that the bulk of the dust mass is cold ($T_{dust} < 30$ K) and radiating beyond 100 μm. Henceforth, we refer to the dust detected by *IRAS* as "warm dust."

Devereux & Young (1990b) considered not only the molecular gas, but also that fraction of the atomic gas associated with the inner disk, i.e. the area within which most of the star formation and hence infrared emission occurs. They find a tight correlation between the warm dust mass measured

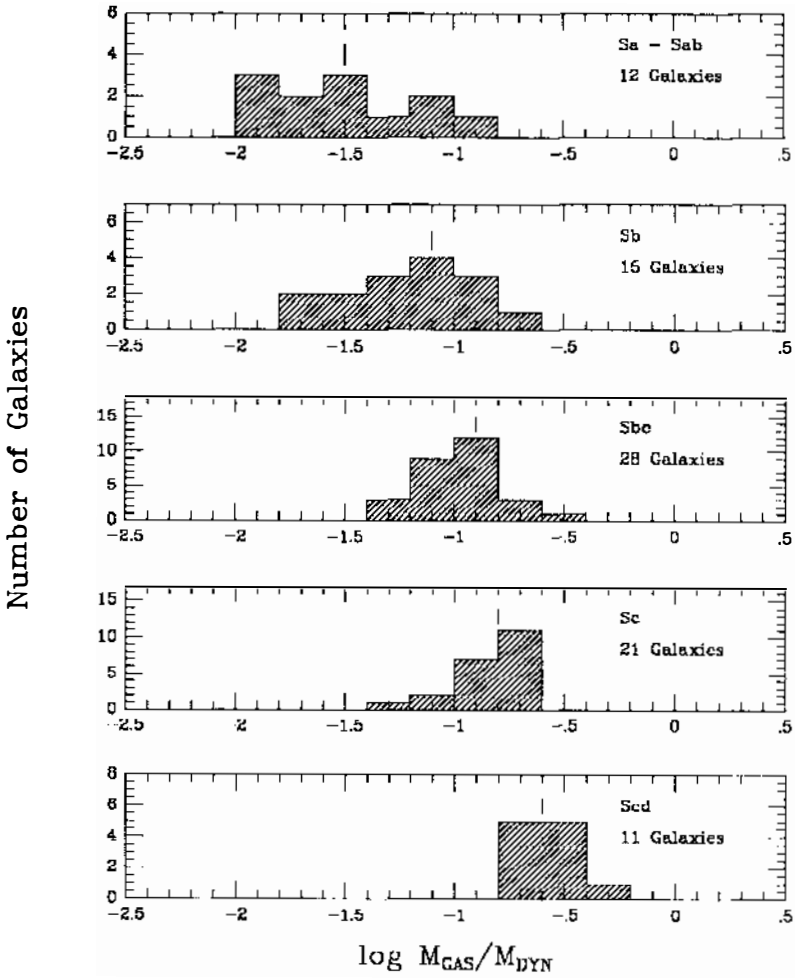

Figure 5 Ratio of total interstellar gas mass (H I + H_2) to dyanimical mass for 150 galaxies (for $H_0 = 50$ km s^{-1} Mpc^{-1}). Dynamical masses were derived by using L_B from RC2 and the results of Rubin et al (1985) for the ratio M_{dyn}/L_B as a function of morphological type. The *vertical tick mark* in each panel represents the median value for that type.

by *IRAS* and the gas mass (H I and H_2) in the inner disk ($R < R_{25}/2$), as shown in Figure 6, and conclude that the warm dust detected by *IRAS* is located in the inner disks and mixed with both H I and H_2 gas. They find the mean inner disk gas-to-warm-dust ratio is $\sim$1000 with no significant variations as a function of morphological type, dust temperature, or

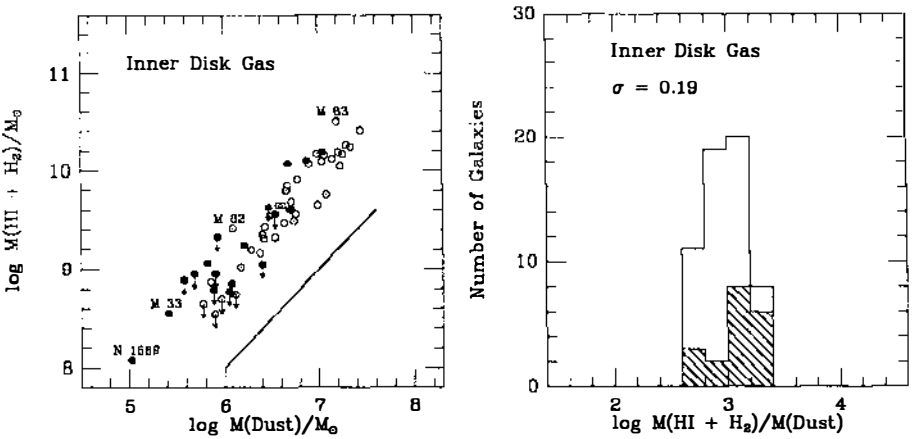

Figure 6 (*Left panel*): Correlation between gas masses in the inner disk ($R < R_{25}/2$) and warm dust masses derived from *IRAS* 60 and 100 μm flux densities (Devereux & Young 1990b). The *open circles* identify galaxies for which the molecular gas constitutes >50% of the gas mass; *filled circles* identify spirals for which atomic gas constitutes >50% of the gas mass. The *solid line* represents gas/dust = 100 and the arrows identify spirals with 2σ upper limits, where the upper limits are due to nondetections of H_2. (*Right panel*): Histogram illustrating the gas/dust ratio. The *shaded portion* of the histogram represents the H I-dominated galaxies. The numerical value of the dispersion is indicated by the value of σ, where the limits have been included in the 2σ value. The similar widths for the histograms of H_2 and H I-dominated galaxies suggest that the H I and H_2 masses have similar accuracy.

whether the H I or H_2 is the dominant phase of the ISM. If the true gas-to-dust ratio in spiral galaxies is the same as the value of $\sim$150 measured within the Galaxy, the high value that is found from this study indicates that 80–90% of the dust mass in spiral galaxies is radiating at $\lambda > 100$ μm and has a dust temperature colder than $\sim$30 K. Furthermore, the small scatter in the gas/dust ratio in Figure 6b is used to argue that the global H_2 masses derived from CO observations and a constant CO-to-H_2 conversion factor have a 1σ uncertainty of $\pm$30% for luminous spiral galaxies (see Section 2.2.2).

6.5 *CO-IR Luminosity Correlation*

A large number of CO-IR comparisons have been reported in the literature (Rickard & Harvey 1984, Young et al 1984, Sanders & Mirabel 1985, Young et al 1986a,b, Sanders et al 1986, 1987, Tacconi & Young 1987, Solomon & Sage 1988, Kenney & Young 1988b, Young et al 1989, Tinney et al 1990, Sanders et al 1991). These correlations exhibit at least an order

of magnitude of scatter, which is much more than that expected on the basis of measurement uncertainties.

Figure 7 shows a plot of the infrared (IR) and CO luminosities for more than 200 galaxies from several studies. The CO luminosities were derived as described in Kenney & Young (1988a), whereas the infrared luminosities are based on coadded *IRAS* data and computed following the method of Lonsdale et al (1985). The values of the ratio $L_{IR}/M(H_2)$ range from 2 to 200 $L_\odot M_\odot^{-1}$, with the higher values occurring in interacting and merging galaxies (see Sections 8–9 and Figure 11) and in starburst irregular galaxies. In Figure 7, where the galaxies are coded by dust temperature, it is clear that the ratio $L_{IR}/M(H_2)$ is closely correlated with dust temperature. Such a separation by dust temperature is not found for the comparison of IR luminosities and H I masses in the IR bright galaxies, thereby strongly

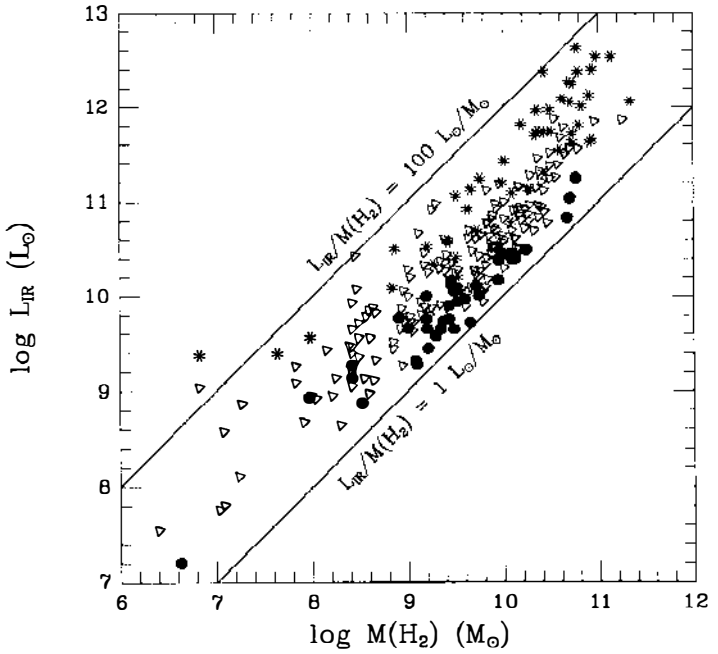

Figure 7 Comparison of total H_2 masses and IR luminosities for galaxies from several studies (Stark 1979, Young et al 1986a, Sanders et al 1986, Tacconi & Young 1987, Solomon & Sage 1988, Kenney & Young 1988a, Young et al 1989, Thronson et al 1989a, Tinney et al 1990, Sanders et al 1991). The H_2 measurements included consist of major axis maps for galaxies larger than 3′, and single observations for the smaller galaxies. *Points* are coded by dust temperature, with *stars* for $T_{dust} > 40$K; *triangles* for T_{dust} between 30 and 40K; and *circles* for $T_{dust} < 30$K. The *diagonal lines* shown represent $L_{IR}/M(H_2) = 1$ and 100 $L_\odot/M_\odot$.

suggesting that the dust emission in these galaxies is more closely tied to the molecular than to the atomic gas content. The correlation of the T_d with the ratio $L_{IR}/M(H_2)$ can be understood, since a higher radiation energy density (i.e. L/M) leads to a higher radiative equilibrium dust temperature.

7. STAR FORMATION RATES AND EFFICIENCIES IN GALAXIES

The rate at which the ISM in a galaxy evolves is determined in large part by the rate of star formation within molecular clouds. The most widely available measures of the star formation activity in galaxies are global Hα fluxes (Kennicutt & Kent 1983, Bushouse 1986, Kennicutt et al 1987) and far infrared fluxes from the *IRAS* survey (Lonsdale et al 1985). Although the Hα emission traces the young stars, the disadvantages of the Hα are several. First, the emission traces only high mass stars so that assumptions about the initial mass function (IMF) must be made in order to deduce the overall star formation rate (SFR). Second, the emission suffers extinction, and will therefore provide only a lower limit to the SFR.

An alternative tracer of the rate of high mass star formation in galaxies is provided by the *IRAS* data. Devereux & Young (1990a) have shown that the global far infrared luminosity observed in spiral galaxies is consistent with that of the high mass OB stars required to ionize the gas. Additionally, only high mass stars are capable of heating the dust in galaxies to the dust temperatures observed throughout spiral disks. In the following, we adopt the view that the SFRs are indicated by the IR luminosities (for a more complete discussion see Devereux & Young 1991). The infrared emission, like the Hα, is nevertheless strongly biased toward the high mass end of the IMF.

From an analysis of the *IRAS* data for 1000 nearby galaxies, Devereux & Young (1991) find that the median high mass SFR is similar for spiral galaxies of types Sa–Scd, while the SFR is an order of magnitude lower for the S0 and Sd–Sm galaxies.

In order to examine the morphological type dependence of the star formation rate per unit mass of gas (or the star formation efficiency, SFE), a number of investigators have determined the $L_{IR}/M(H_2)$ ratio for early and late type spirals. Rengarajan & Verma (1986), Young et al (1989), Thronson et al (1989b), Wilkind & Henkel (1989), Devereux & Young (1991) and Allen & Young (1989) all find that early and late type spirals have similar global SFEs, as shown in Figure 8. Thus, the *global* star formation rates and efficiencies in disk galaxies do not depend strongly

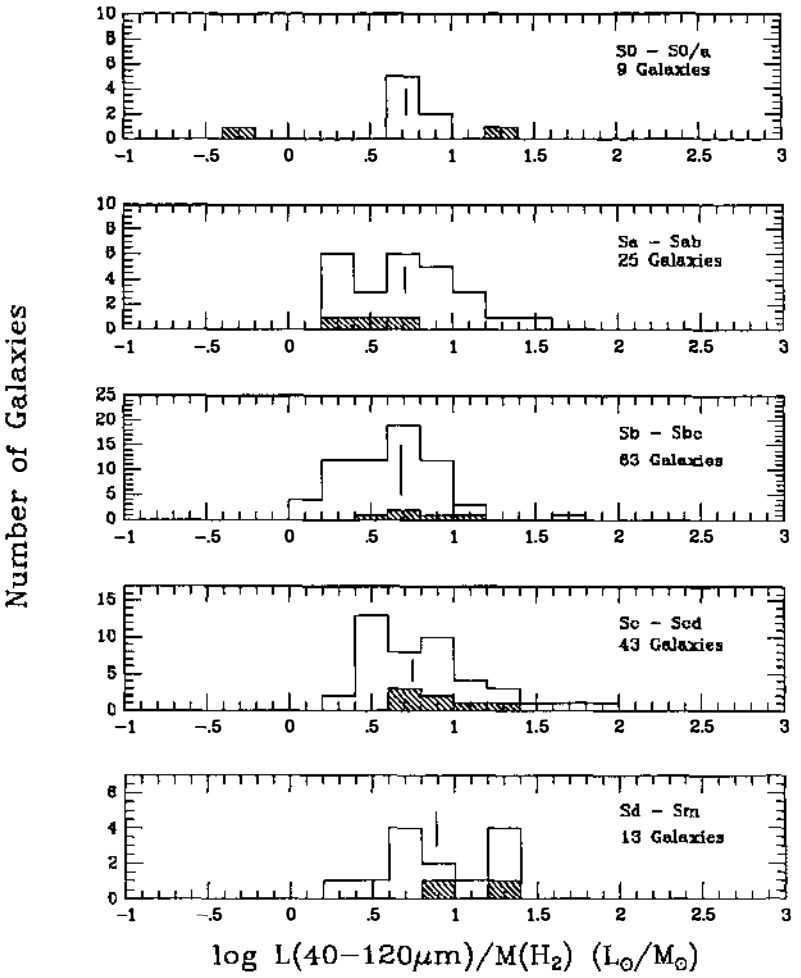

Figure 8 Histograms of the ratio $L_{IR}/M(H_2)$ for each morphological type among spiral galaxies. The *vertical tick mark* in each panel represents the median value of $L_{IR}/M(H_2)$ for that type. The *hatched portion* of each histogram represents galaxies with H_2 upper limits, and $L_{IR}/M(H_2)$ lower limits. The constancy of $L_{IR}/M(H_2)$ in the mean for spiral galaxies along the Hubble sequence indicates that the global star formation efficiency does not change with type.

on morphology. Global SFEs do, however, depend on environment as discussed in Section 8.

If the present high mass star formation rate in spiral galaxies remains constant, then the molecular ISM will be cycled into high mass stars

($\gtrsim 5\,M_\odot$) on a time scale of 10^9 yrs. Needless to say, the gas used in the formation of high mass stars is returned to the ISM via supernova explosions. Consequently, the concern over short gas depletion time scales depends largely on the low mass star formation rate, which is poorly determined at present.

7.1 *The Star Formation Efficiency in the Disks of NGC 6946 and M51*

A complementary approach to understanding galaxy evolution is to compare the detailed distributions of the star formation tracers within the disks of individual galaxies. From a comparison of the CO distribution with past (blue light) and present (Hα or IR) tracers of star formation, one can qualitatively infer the history of the star formation. NGC 6946 (Scd) is a nearby face-on spiral galaxy that is ideal for comparing the distributions of young stars and gas within both the disks and the spiral arms. It is also isolated, with no significant companions within 1 Mpc.

In NGC 6946, the azimuthally averaged distributions—FIR, blue light, Hα, radio continuum, and CO (see Tacconi & Young 1986 for references)—show the same radial fall-off (Figure 9), which is unlike that of the atomic gas. If the blue light measures the star formation rate integrated over the last $\sim 2 \times 10^9$ years (cf. Searle et al 1973, Gallagher et al 1984, Sandage 1986), and the Hα flux measures the current rate of formation of high mass stars, the fact that the blue/CO and Hα/CO ratios are constant as a function of radius indicates that both the present-day formation rate for high mass stars and the long-term integrated formation rate for intermediate mass stars are proportional to the available supply of molecular gas; i.e. the star formation efficiency is approximately constant.

In NGC 6946 (and most other luminous spiral galaxies), the H_2 and H I radial distributions are entirely different. If the ratio of H_2/H I surface densities is taken as a measure of the efficiency with which molecular clouds form, the radial decrease in the H_2/H I ratio indicates that molecular cloud formation proceeds most efficiently or that the clouds last longer toward the center of the galaxy. Inefficient molecular cloud formation in the outer parts of galaxies could result in part from decreasing gas volume densities as the H I scale height increases (Mihalas & Binney 1981).

Models for the star formation *efficiency* within galactic disks have been proposed by Gusten & Mezger (1982) and Dopita (1985). The density-wave model of Gusten & Mezger predicts that the SFE should depend on the difference between the angular velocity and the pattern speed, $[\Omega(R)-\Omega_p]$, which decreases as a function of radius. Dopita's model also depends on the pressure of the ISM and predicts a SFE that is proportional to the stellar surface density, also decreasing with radius. The predictions of these models have been compared with the observationally

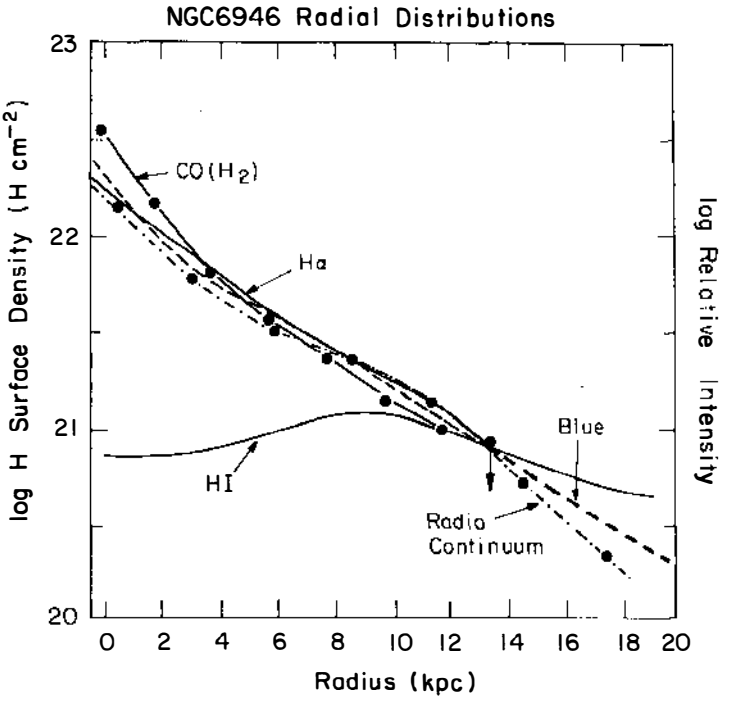

Figure 9 Comparison of the radial distributions of CO (H_2), H I, Hα, blue and radio continuum in NGC 6946 from Tacconi & Young (1986). References are given in Tacconi & Young (1986).

derived SFE for M51 (Lord & Young 1990), but neither model accounts for the apparent constancy of the SFE with radius.

7.2 *Arm-Interarm Variations*

Azimuthal variations in NGC 6946 and M51 have been analyzed with the goal of determining the ratio of young stars to gas and H_2/H I in spiral arm and interarm regions (Lord 1987, Tacconi 1987, Tacconi & Young 1990, Lord & Young 1990). Figure 10 shows the distributions of H_2, H I, Hα, B-, and I-band light, Hα/H_2, H_2/H I, and Hα/blue as a function of azimuth in NGC 6946 at a radius of 1.5′. At this radius, the Hα arms at 45″ resolution stand out as a factor of ~4 enhancements relative to interarm locations; in CO at this resolution, the spiral arms are much less apparent. Thus, the yield of massive stars per unit mass of molecular gas in NGC 6946 is cnhanced by more than a factor of 2 on the spiral arms relative to the interarm regions. Tacconi & Young find the arm-interarm

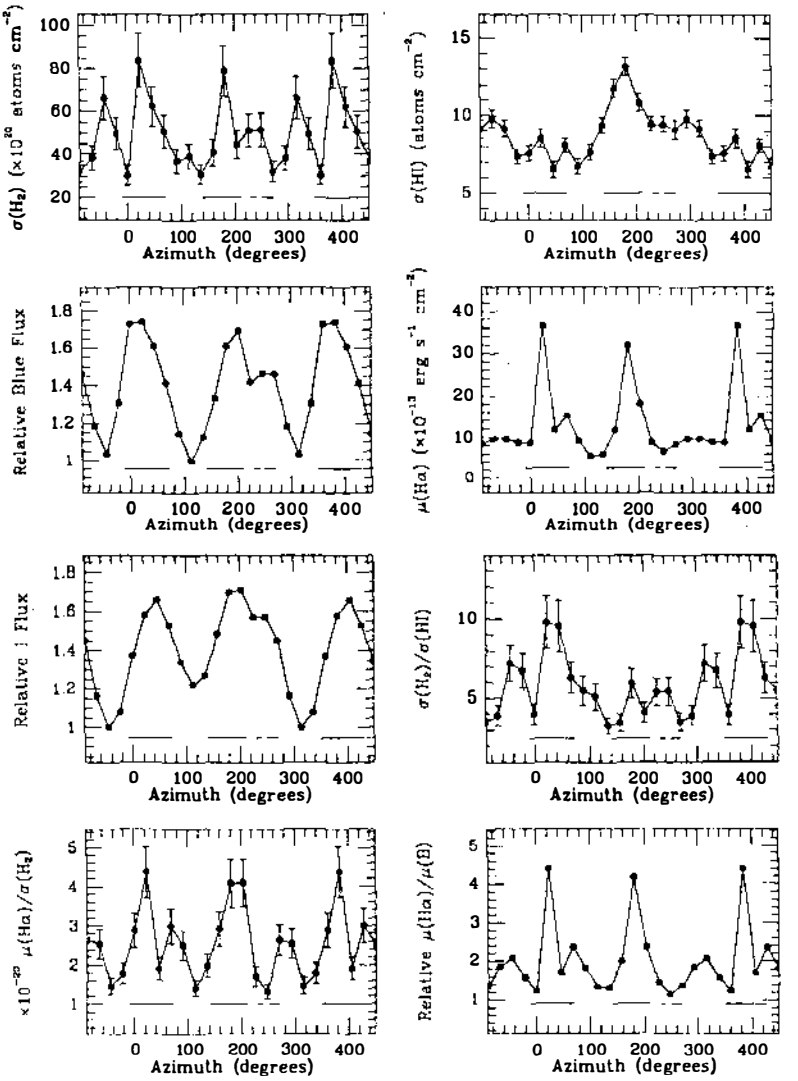

Figure 10 Azimuthal distributions of H_2, H I, Hα, B-band, I-band, Hα/H_2, H_2/H I, and Hα/blue at a radius of 1.5′ in the disk of the Scd galaxy NGC 6946 from Tacconi & Young (1990), all derived at 45″ resolution. Azimuths are defined from north through east, with north at 0°. The *solid horizontal lines* in the lower portion of each panel indicate the locations of the I-band spiral arms before smoothing the data to 45″ resolution. The Hα/H_2 ratio as a function of azimuth shows enhancements in the spiral arm regions indicating that the star formation *efficiency* is a function of the H_2 density.

contrast in the $H\alpha/H_2$ to increase with radius to a value that exceeds 10 beyond a radius of 2′.

Like NGC 6946, M51 also exhibits a factor of ~2 enhancement in the star formation efficiency on the spiral arms (Lord 1987, Vogel et al 1988, Lord & Young 1990). In particular, Vogel et al (1988) inferred arm/interarm contrasts of 2–5 in CO and 10 in Hα on scales of ~500 pc. A similar arm/interarm contrast was measured for CO in M51 by Garcia-Burillo & Guelin (1990). These studies indicate that the yield of high mass stars per unit H_2 mass in spiral arms of luminous Sc galaxies is enhanced relative to the interarm regions by at least a factor of 2.

The elevated Hα/CO ratios associated with spiral arm gas concentrations indicate that there is a nonlinear dependence of the OB star formation rate on the local gas surface density. The variations on and off the spiral arms in NGC 6946 and M51 are consistent with the *high mass* SFR depending quadratically on the H_2 surface density. Based on a similar increase in the number of radio H II regions relative to the density of GMCs in the spiral arms of the Galaxy, Scoville et al (1986a) suggested that OB star formation may be linked to the collisions of GMCs. A bias for the formation of *high* mass stars during cloud-cloud collisions could arise, since the gas will be shock heated and the first stars to form as the gas cools would be high mass stars (cf. Silk 1987). It is not clear whether the IMF within the arms is biased toward high mass stars, or whether more stars of all masses form in these regions. We suspect that there may well be separate modes of star formation for low and high mass stars (cf. Larson 1987). Perhaps the low mass star formation *rate* depends linearly on the gas density and the high mass mode quadratically.

How is it, then that the azimuthally averaged Hα and CO radial distributions are so similar in NGC 6946 (and M51), while the Hα shows greater enhancement on the spiral arms? This inconsistency could be resolved if the spiral arms comprise a small fraction of the surface area of a galaxy and only a small fraction of the total molecular gas and Hα resides in the arms. Thus, spiral arms are best studied by investigating gas and star formation as a function of azimuth, whereas azimuthal averaging reveals the characteristics of the underlying disk.

8. GALACTIC INTERACTIONS

Galaxy-galaxy interactions are known to disrupt the stellar component of disks (Toomre & Toomre 1972), and to enhance the star formation rate (cf. Larson & Tinsely 1978, Lonsdale et al 1984). Through investigations of the molecular content along with the star formation rate, we now have a handle on the star formation efficiency in interacting galaxies.

8.1 *Star Formation Efficiencies*

Several studies have investigated the star formation efficiency in interacting/merging galaxies (Sanders & Mirabel 1985, Young et al 1986a,b, Solomon & Sage 1988, Sanders et al 1991, Tinney et al 1990) and found that *strongly* interacting galaxies have mean $L_{IR}/M(H_2)$ ratios 5–10 times higher than isolated galaxies. A similar enhancement is found in the $L_{H\alpha}/M(H_2)$ ratios for interacting/merging galaxies versus isolated galaxies (Allen & Young 1989). Most of the studies have also indicated that only the most closely interacting systems have a significant enhancement. These results suggest that the perturbations due to galaxy-galaxy interactions result in more efficient production of massive stars.

Figure 11 shows a plot of the ratio $L_{IR}/M(H_2)$ versus dust temperature for 150 galaxies, in which the points are coded by the galaxy's environment (dwarf irregulars, isolated, group/cluster, and interacting/merging gal-

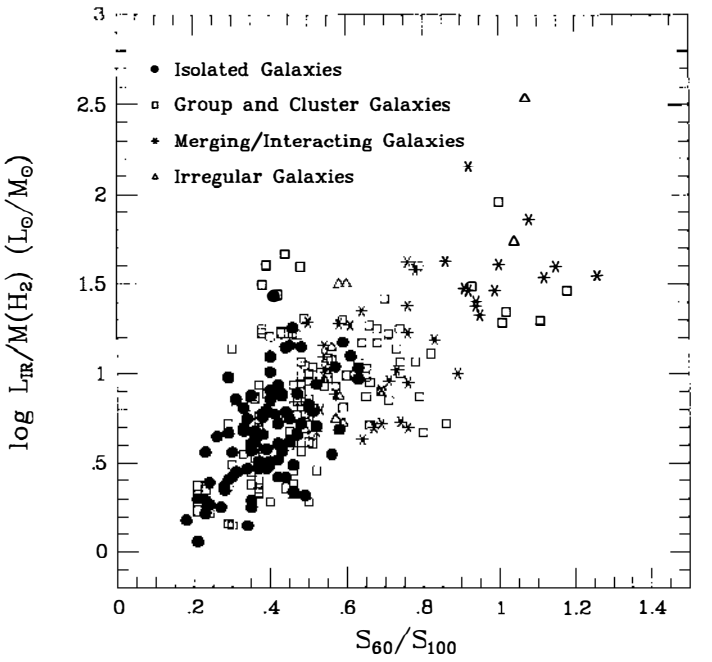

Figure 11 Comparison of the ratio $L_{IR}/M(H_2)$ with S_{60}/S_{100} for the galaxies in Figure 7. The galaxies are coded by environment as follows: *filled circles* for isolated galaxies, *open squares* for group and cluster galaxies, *stars* for interacting/merging galaxies, and *open triangles* for dwarf and irregular galaxies. The merging/interacting galaxies have high values of both $L_{IR}/M(H_2)$ and S_{60}/S_{100} relative to the isolated galaxies.

axies). Although the most strongly interacting galaxies often have high star formation efficiencies, there is an order of magnitude scatter in the L/M observed among both the isolated and interacting galaxies. This scatter, which is considerably larger than the measurement uncertainties ($\pm 30\%$), may reflect time evolution of the IR luminosity and/or the H_2 content for the starbursts in the interacting galaxies (Young et al 1986a,b). Scalo (1987) has suggested that bursts of star formation control the evolution even in isolated galaxies, and this might account for the large scatter in the star formation efficiency for the normal galaxies.

Several mechanisms for the enhancement in the yield of young stars per unit mass of molecular gas in interacting/merging galaxies have been suggested. On one hand, the galaxy-galaxy interaction may cause a new star formation mechanism to operate such that more stars form per unit molecular mass. Alternatively, the physical process that causes high mass stars to form in merging/interacting galaxies may be no different than that in isolated galaxies, but the interaction may enhance its effectiveness. We favor the latter explanation, i.e. the interaction causes a star formation mechanism already present to operate at an increased level, as opposed to invoking a new mechanism.

One process that probably becomes important during galaxy-galaxy interactions is that of cloud-cloud collisions. Noguchi & Ishibashi (1986) and Olsen & Kwan (1990) have performed numerical simulations of galaxy-galaxy interactions including gas clouds as well as stars. They find that the cloud-cloud collision rate increases as bridges and tails develop during violent galaxy-galaxy encounters. In the specific cases treated by Noguchi & Ishibashi, the cloud collision rate is elevated by an order of magnitude at 3×10^8 years after the closest approach of the perturber. If cloud-cloud collisions are responsible for high mass star formation galaxies (Scoville et al 1986a), the enhanced rate of cloud-cloud collisions in interacting galaxies should result in an increase in the star formation rate per unit H_2 mass.

8.2 *Interaction Morphology*

One of the interacting systems for which the most complete data exist and for which extensive dynamic modeling has been done is the "antennae" system, NGC 4038/39 ($D = 20$ Mpc for $H_0 = 75$ km/s/Mpc). Knots of intense Hα emission are found throughout both galaxies (Rubin et al 1970), and a total molecular gas mass of 5.3×10^9 $M_\odot$ (Young et al 1989) is seen distributed throughout this system. Aperture synthesis at 6″ resolution of the CO emission has recently been reported by Stanford et al (1990). The integrated CO intensity contours are shown in Figure 12 superposed on a 6500 Å image of the inner region of this system. Three concentrations of CO emission are evident: Two are centered near the

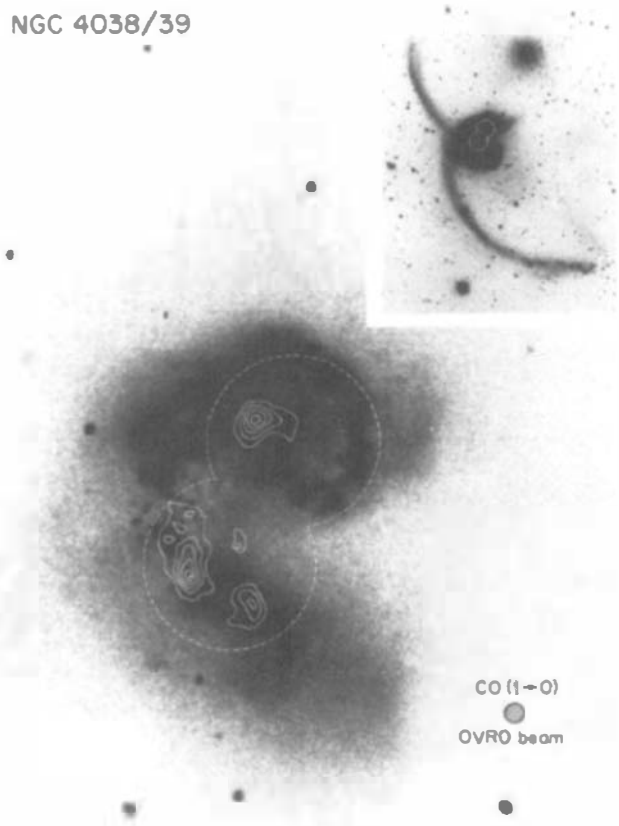

Figure 12 CO integrated intensity maps in two interferometer fields are overlaid on an R band image of Arp 244 (NGC 4028/39), the "Antennae" system (Stanford et al 1990). The inset is a large scale, deep exposure of the galaxies. The northern and southern CO concentrations coincide with the nuclei of NGC 4038 and NGC 4039; the eastern emission complex is at the interaction interface of the two galaxies. Contour levels are 5, 10, 20, 30, 40, 50, 60, 70, 80, and 90% of the peak flux (89 Jy km s^{-1} $beam^{-1}$).

nuclei of NGC 4038 and NGC 4039, closely correlated with Hα and radio continuum peaks; a third CO emission region lies about 25″ northeast of the NGC 4039 nucleus where the two galaxies overlap. The masses of these molecular gas concentrations are in the range 0.2–1.2 $\times$ 10^9 $M_\odot$. If the results obtained in this system are representative, it appears that a galactic collision such as is occurring in this system may result in a large mass of gas concentrating in the nucleus and in the region of direct overlap of the galactic disks. Similar characteristics are found for the CO emission in Arp 299 (IC 694/NGC 3690) (Sargent et al 1987, Sargent & Scoville 1991).

Both the "Antennae" system and Arp 299 may be in an intermediate phase of galactic interaction; examples of more advanced mergers may be found in the ultraluminous *IRAS* galaxies (Section 9.3).

9. GALACTIC NUCLEI

In the center of our Galaxy, the predominant gas phase is molecular and a total H_2 mass of approximately $1–5 \times 10^8$ $M_\odot$ is estimated for the inner 800 pc radius. The dominant large-scale morphological feature is an expanding ring or arms at approximately 200–300 pc radius, made up of extremely massive clouds ($\gtrsim 10^6 M_\odot$). The mean gas densities in these clouds are at least a factor of 10 higher than those of typical Galactic GMCs.

In all but the nearest external galaxies, high resolution observations are required to detect the existence of such structures, if they exist. Three of the nearby spiral galaxies (IC 342, NGC 6946, and NGC 253) for which aperture synthesis observations have been obtained, exhibit elongated bar-like distributions for the molecular gas in the central kpc (Section 3.2). In three other nearby galaxies studied at high resolution (Maffei 2, NGC 2146, and NGC 3079), elongated distributions are also seen in the nuclei, but these galaxies are observed at high inclination, and the observed structures may simply be inclined nuclear disks (Nakai et al 1989, Young et al 1988a,b, Jackson & Ho 1988). In the center of M51 (see Figure 3), there is an apparent deficiency of molecular gas within the central 600 pc (Lo et al 1987b, Rand & Kulkarni 1990). Two galaxies analyzed in considerably greater detail are the nearby irregular galaxy M82 and the Seyfert II galaxy NGC 1068.

9.1 *M82*

M82 is one of the first galaxies in which CO was detected (Rickard et al 1975, Solomon & de Zafra 1975), and the CO emission in this nearly edge-on irregular galaxy has been mapped extensively (see Table 2 for references). The total H_2 mass within the inner 6 kpc could be as high as 2×10^9 $M_\odot$ (assuming the standard galactic CO to H_2 conversion), in which case, it is an order of magnitude greater than the H I mass within the same region. It is one of the few galaxies in which the molecular emission is sufficiently bright to enable studies of molecules other than CO. Rickard & Palmer (1977) first detected HCN and CS here. In addition, ^{13}CO $J = 1–0$ is observed with an intensity approximately 1/20 that of CO (Stark & Carlson 1984, Young & Scoville 1984), and the CO $J = 2–1$ emission is significantly brighter than the $J = 1–0$ emission at the central position (Knapp et al 1980, Sutton et al 1983). Both of these characteristics

have led a number of authors to suggest that the CO emission in the center of M82 is optically thin, an excitation regime seldom seen in galactic GMCs.

Carlstrom (1988) has publishcd high resolution aperture synthesis maps of the CO, HCO^+, HCN, and 3 mm continuum emission, as shown in Figure 13 together with the 6 cm and 2 μm continuum. The 2 μm continuum arises mostly from late-type giant stars; the 6 cm continuum is mainly synchrotron emission from high energy particles injected into the ISM from supernovae; and the 3 mm continuum is predominately free-free emission from H II regions, ionized by young stars. All of the distributions show an elongation of the central galactic disk, and within the disk all of

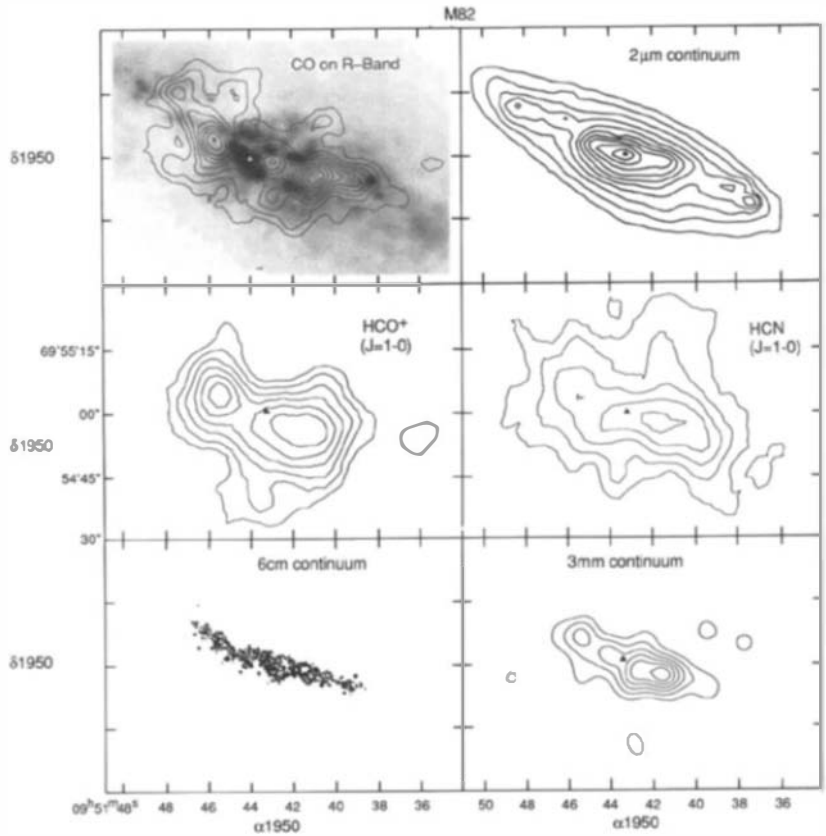

Figure 13 The central disk of M82 with CO (5.5″ resolution) on an R-band gray scale image; the 2 μm continuum (Telesco et al 1990); HCO^+ (10″ resolution); HCN (10″ resolution); 6-cm radio continuum (0.35″ resolution, Kronberg et al 1985); and 3 mm continuum (6″ resolution). The *diamond* denotes the position of the 2 μm "stellar" peak. The molecular images and the 3 mm continuum are from Carlstrom (1988).

the molecular line maps show a clear double-peaked structure. The latter feature was first discovered by Nakai et al (1987) and is generally interpreted as an edge-on torus at 200 pc radius. The total mass of gas in this structure is 0.6–1 $\times$ 10^8 $M_\odot$, which is 10% of the dynamical mass within the same region. The central peak in the 2 μm continuum probably represents the nuclear star cluster with a significant enrichment by super-giant stars produced from the starburst. It is noteworthy that the distribution of nonthermal radiation shown in the 6 cm continuum shows roughly the same spatial extent as the molecular torus, but no evidence of the two peaks seen in the molecular emission. Comparison of the 3 mm continuum map with the distribution of gas seen in the CO, HCO^+, and HCN suggests that at present, the formation of high mass stars as probed by the distribution of free-free emission is occurring predominately to the west of the nucleus.

Based upon an excitation analysis of the HCN and HCO^+ emission, Carlstrom finds that the density of the gas in the emitting regions probably exceeds 5 $\times$ 10^4 cm^{-3}, that is, a factor of 200 higher than the mean volume densities of galactic GMCs. This dense gas has a filling factor $\lesssim$0.1%. The Lymann continuum production rate required to explain the 3 mm free-free emission is 6 $\times$ 10^{53} sec^{-1} (Carlstrom 1988), exceeding by a factor of four the Lyman continuum production rate required for the entire Milky Way (Mezger 1978). The implied rate of star formation within the molecular torus is $\dot{M} \simeq$ 6–10 $M_\odot$ yr^{-1} assuming a Miller-Scalo initial mass function with an upper mass cutoff of 45 $M_\odot$ and lower mass cutoffs of 0.1–1 $M_\odot$ (see Scoville & Soifer 1991). At this rate, the gas in the torus at 200 pc radius would be entirely converted into stars in 10^7 years (if low mass stars do indeed form) and in order to maintain the nuclear starburst, gas must flow in from further out in the galaxy. If low mass stars do not form, the starburst can be sustained for a considerably longer time.

9.2 *NGC 1068*

NGC 1068 is the nearest galaxy with both a Seyfert II active nucleus and a high rate of star formation in its inner disk. Half of the total luminosity (2 $\times$ 10^{11} $L_\odot$) originates from an extended disk of young stars at radii $<$1.5 kpc (Telesco & Harper 1980); the remainder arises in a source $<$0.5″ in size, centered on the Seyfert nucleus. This galaxy has been the focus of numerous molecular line studies (see Table 1), with the highest resolution corresponding to 260 pc.

In Figure 14, the integrated CO emission at 2.9″ resolution is shown superposed on a U-band optical image (Planesas et al 1991). Two spiral arms of molecular gas are seen encircling the nucleus at a radius of approximately 1.5 kpc, with many distinct emission complexes of size up to 500 pc and masses up to 7 $\times$ 10^8 $M_\odot$. The arms, containing a total H_2

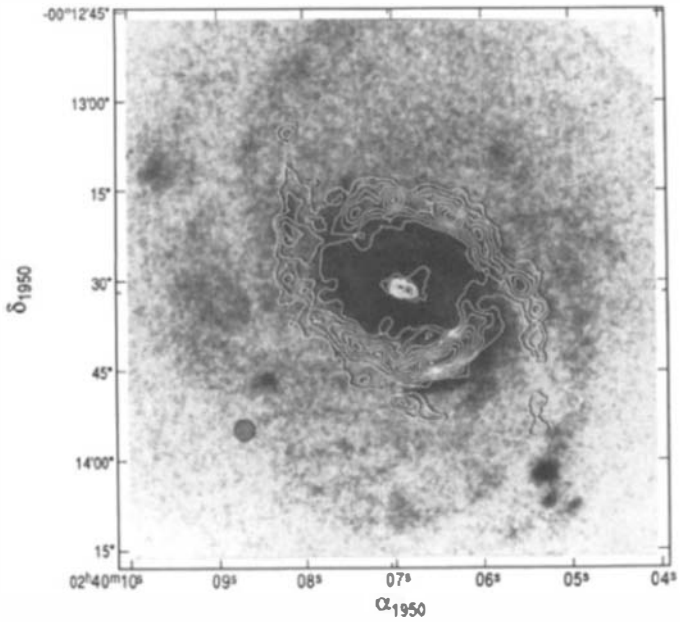

Figure 14 Map of the integrated CO emission in NGC 1068 overlaid on a U-band image of the inner region of the galaxy (Planesas et al 1991). The major features seen in CO are the inner spiral arms ($\sim 5 \times 10^9$ $M_\odot$) of molecular gas at $\sim 15''$ radius (1.5 kpc), which originate from the ends of the central stellar bar and a compact source ($\sim 3''$) coincident with the Seyfert 2 nucleus.

mass of 5×10^9 $M_\odot$, originate at the outer ends of a stellar bar seen in the near infrared (Scoville et al 1988, Thronson et al 1989c). The kinematics of the molecular ring can be fit by circular rotation if the position angle of the major axis is 90° or by rotation plus expansion if the major axis position angle is taken as 40° (Planesas et al 1991).

In Figure 14, an emission peak may also be seen coincident with the Seyfert nucleus. Although approximately half of this emission is radio continuum from the central non-thermal source, the remainder is probably CO emission. The total mass of H_2 in the nuclear source at a radii <130 pc is approximately 8×10^7 $M_\odot$. The dust associated with this gas may be responsible for obscuring the direct line of sight to the Seyfert I nucleus hypothesized on the basis of optical spectropolarimetry (Antonucci & Miller 1985).

9.3 *Ultraluminous Infrared Galaxies*

Perhaps most dramatic in starburst activity are the ultraluminous ($L_{IR} > 10^{12}$ $L_\odot$) galaxies highlighted by the *IRAS* survey. At the highest

luminosities, one sees a preponderance of galaxies with double nuclei and/or extended tidal tails indicative of galactic interactions or the merging of two galaxies (Sanders et al 1988c). The optical spectra of the ultraluminous galaxies are dominated by emission line ratios characteristic of a narrow line AGN or Seyfert nucleus rather than the thermal, H II region, line ratios seen in lower luminosity galaxies. This qualitative assessment of the optical data strongly suggests that the highest luminosities are initiated by galactic collisions, and the energy is supplied probably by the combination of an extremely energetic starburst and an embedded, nonthermal AGN.

Virtually all of the luminous *IRAS* galaxies have been shown to be extremely rich in interstellar gas, predominantly molecular hydrogen (see Figure 9). This gas is also highly concentrated in the nuclei of the galaxies. Over the last four years, aperture synthesis maps have been made of the CO emission in approximately 25 of the luminous and ultraluminous infrared galaxies (Scoville et al 1986b, 1989, 1991; Sargent et al 1987, Sargent & Scoville 1991, Sanders et al 1988a, Meixner et al 1990, Ishizuki et al 1990). The results for 18 of these systems are summarized in Scoville et al (1991). In most cases the size of the CO-emitting region is $\lesssim 1$ kpc in radius, and the masses of molecular gas in the nuclear sources are 10^9–4×10^{10} $M_\odot$ (assuming the Galactic CO-to-H_2 conversion factor). The galaxies span the luminosity range 2×10^{10} $L_\odot$ to 3×10^{12} $L_\odot$ (for $\lambda = 8$–1000 μm), and the global infrared luminosity-to-total-molecular mass ratios range from 4 $L_\odot/M_\odot$, like the Milky Way, to 200 $L_\odot/M_\odot$ for Mrk 231.

Scoville et al (1991) computed the gas mass fraction (M_{H_2}/M_{dyn}) for those galaxies in which the nuclear mass concentration is resolved and for which the velocity dispersion can be estimated from the CO line-width. For the six cases in which this ratio has been evaluated, the interstellar gas constitutes a significant fraction of the total mass in the nucleus. This is consistent with numerical simulations of merging galaxies (Hernquist 1989) including a gas component. The simulations show that the gas sinks to the center of the merged system more readily than the stellar component because gas is much more dissipative than the stars.

Virtually all of the very luminous infrared galaxies show evidence of a significant galactic interaction (cf. Sanders 1990). The interstellar matter can play a central role in the dynamics of a galactic interaction, since the gas is dissipative and hence responds irreversibly to the perturbation, sinking toward the center of the potential well. The H_2 masses for the luminous infrared galaxies are large but, in most cases, not more than would be found in two galaxies such as M51 or M83 ($M_{H_2} \sim (1$–$3) \times 10^{10} M_\odot$). In most cases, it is therefore plausible that the luminous infra-

red galaxies result from the merging of two gas-rich spiral galaxies, and that the disturbed dynamics in the merging system results in dissipation of kinetic energy (and outward transport of angular momentum) in the ISM, thus leading to the deposition of a significant fraction of the original interstellar matter in the central region of the system. There, binary processes such as cloud-cloud collisions or stimulated star formation can enhance the overall efficiency and rate of conversion of interstellar gas into young stars.

Arp 220, the prototype ultraluminous infrared galaxy, has an infrared luminosity at $\lambda = 8$–$1000\ \mu$m of $1.5 \times 10^{12}\ L_\odot$, exceeding that in the visual by nearly 2 orders of magnitude and placing it in the luminosity regime of quasars. Single dish measurements show the CO emission extending over a velocity range of 900 km s^{-1}, and the derived H_2 mass is $3.5 \times 10^{10}\ M_\odot$, approximately a factor of 15 greater than that of the Galaxy (Solomon et al 1990). At optical wavelengths, the galaxy appears approximately spherical with a central dust lane and tidal tails, both characteristics of galactic merging, extending up to 70 kpc away (Sanders et al 1988c). The CO emission, observed at 2″ resolution (Scoville et al 1991), can be separated into two components: a core $1.4 \times 1.9''$ and an extended component $7 \times 15''$ containing 2/3 and 1/3 of the flux, respectively. For the adopted distance of 77 Mpc (for $H_\circ = 75$ km s^{-1} Mpc^{-1}) the H_2 masses in the core and extended components are $1.8 \times 10^{10}\ M_\odot$ and $9 \times 10^9\ M_\odot$, respectively. The mean diameter of the core component ($\sim 1.7''$) corresponds to a radius of 315 pc, and the H_2 density, smoothed out over the volume, is 2900 cm^{-3}. Solomon et al (1990) deduced a higher density (10^4–10^5 cm^{-3}) based on CS measurements. Within the core source of radius 315 pc, the dynamical mass is $\gtrsim 2.5 \times 10^{10}\ M_\odot$, i.e. almost precisely equal to the total gas mass (H_2+He) derived from the CO line flux for the core component.

9.4 *Quasars*

Many of the properties of the ultraluminous galaxies (luminosity, nonthermal optical emission line ratios, and spectral energy distributions) are similar to those of previously identified optical quasars. The detection of CO emission in Mrk 231 (Sanders et al 1987) stimulated a search for CO emission in normal optical quasars, since Bokensburg et al (1977) had speculated on the basis of the optical emission lines that this galaxy might harbor a dust-embedded quasar. Most spectacular are the detections of CO emission in the optical quasars IZw1 and Mrk 1014 (Barvainis et al 1989, Sanders et al 1988b), the latter at a redshift of 47,000 km s^{-1} ($z = 0.17$). These detections are not just impressive in their own right, but also potentially of great importance to our understanding of the

evolutionary circumstances that lead to AGNs and quasars. Recently, Alloin et al (1991) have reported the detection of CO in the quasar E1821+643 at a redshift of 0.30. If this detection is confirmed, the measured CO luminosity indicates a total H_2 content exceeding 10^{11} $M_\odot$.

Scenarios elucidating a sequence of events whereby gas-rich galactic mergers promote the evolution of a nuclear starburst cluster to form a central AGN have been put forward by David et al (1987), Norman & Scoville (1988), and Hernquist (1989). In these models, the standard optical quasar represents a phase subsequent to the gas-rich nuclear starburst. In the early evolution of such mergers, the bulk of the luminosity is emitted in the far infrared due to the large abundance of interstellar dust; however, the high luminosity generated by the nuclear starburst and by accretion onto the AGN will eventually disperse the interstellar gas and dust, leaving a normal optical quasar.

10. CONCLUSIONS

The explosive growth of molecular line observations (primarily CO) in galaxies over the last decade have provided a detailed characterization of the dense interstellar medium and its relationship to star formation in galaxies. The total H_2 content of approximately 400 galaxies has now been determined, and characterizations of the H_2, H_2/H I, L_*/H_2, and gas mass fraction as a function of morphological type, galactic luminosity, and environment are becoming well established. In addition, high resolution studies in recent years have at last provided the spatial resolution to define the role of molecular gas in spiral structure and starburst galactic nuclei.

Major advances are anticipated for the next decade from radically improved instrumental capabilities. The very large aperture single dish telescope will enable detection of CO emission from gas-rich galaxies out to $z \sim 1$ and perhaps enable detection of true protogalactic objects. The greatly increased speed and sensitivity expected for millimeter-wave aperture synthesis arrays should provide a similar explosive increase in high resolution imaging of galaxies. The order of magnitude increase in speed expected for focal plane arrays in conjunction with single dish telescopes will provide the unique capability of imaging large, nearby galaxies. Lastly, observations at submillimeter wavelengths will enable more detailed analysis of the physical conditions in the molecular gas from multitransition studies and high resolution observations of the far infrared continuum.

ACKNOWLEDGMENTS

It is a pleasure to acknowledge the extensive work of Leona Kershaw in preparation of this manuscript. The authors wish to thank Drs. Nick

Devereux and Dave Sanders for helpful discussions. This work is supported in part by NSF Grants AST 88-15406 (J. Y.) and AST 87-14405 (N. S.). J. Y. also wishes to thank the JCMT and University of Hawaii for generous support during the completion of this manuscript.

Literature Cited

Adler, D., Liszt, H. 1989. *Ap. J.* 339: 836
Allen, L., Young, J. S. 1989. In *2nd Teton Conf. on ISM in Galaxies*, ed. H. Thronson, M. Shull. Dordrecht: Klower
Allen, R. J., Atherton, P. D., Tilanus, R. P. J. 1986. *Nature* 319: 296
Alloin, D., Barvainis, R., Antonucci, R., Gordon, M. 1991. *Astr. Ap.* In press
Antonucci, R., Miller, J. 1985. *Ap. J.* 297: 621
Arnault, P., Casoli, F., Combes, F., Kunth, F. 1988. *Astr. Ap.* 205: 41
Ball, R., Sargent, A., Scoville, N., Lo, F., Scott, S. 1985. *Ap. J. Lett.* 298: L21
Barvainis, R., Alloin, D., Antonucci, R. 1989. *Ap. J. Lett.* 337: L69
Becker, R. 1990. PhD thesis, Univ. Bonn
Becker, R., Schilke, P., Henkel, C. 1989. *Astr. Ap.* 211: L19
Bieging, J., Blitz, L., Lada, C., Stark, A. 1981. *Ap. J.* 247: 443
Bloemen, J. B. G. M., Strong, A., Blitz, L., Cohen, R. S., Dame, R. S. et al. 1986. *Astr. Ap.* 154: 25
Boksenberg, A., Carsuck, R. F., Allen, D. A., Fosbury, R. A. E., Penston, M. V., Sargent, W. L. W. 1977. *MNRAS*, 178: 451
Boulanger, F., Bystedt, J., Casoli, F., Combes, F. 1984. *Astr. Ap.* 140: L5
Brand, J., Aouterloot, J., Becker, R., Stripe, G. 1989. *Astr. Ap.* 211: 315
Brinks, E. 1985. PhD thesis, Sterrewacht Leiden
Brouillet, N., Baudry, A., Combes, F., Kaufman, M., Bash, F. 1990. *Astr. Ap.* In press
Bushouse, H. 1986. PhD thesis, Univ. Illinois
Canzian, B. 1990. PhD thesis, Calif. Inst. Technol.
Canzian, B., Mundy, L., Scoville, N. 1988. *Ap. J.* 33: 157
Carlstrom, J. 1988. PhD thesis, Univ. Calif., Berkeley
Casoli, F., Combes, F., Dupraz, C., Gerin, M., Encrenaz, P., Salez, M. 1988. *Astr. Ap.* 192: L17
Casoli, F., Clausset, F., Viallefond, F., Combes, F., Boulanger, F. 1990. *Astr. Ap.* 233: 357
Casoli, F., Combes, F. 1988. *Astr. Ap.* 198: 43
Casoli, F., Combes, F., Augarde, R., Fijon, P., Martin, J. M. 1989. *Astr. Ap.* 224: 31
Cohen, R. S., Dame, T., Garay, G., Montani, J., Rubio, M., Thaddeus, P. 1988. *Ap. J. Lett.* 331: L95
Combes, F., Dupraz, C., Casoli, F., Pagani, L. 1988. *Astr. Ap.* 203: L9
Combes, F., Encrenaz, P. J., Lucas, R., Weliachew, L. 1977a. *Astr. Ap.* 55: 311
Combes, F., Encrenaz, P. J., Lucas, R., Weliachew, L. 1977b. *Astr. Ap.* 61: L7
Combes, F., Encrenaz, P. J., Lucas, R., Weliachew, L. 1978. *Astr. Ap.* 63: L13
Combes, F., Gerin, M. 1985. *Astr. Ap.* 150: 327
David, L. P., Durisen, R. H., Cohn, H. 1987. *Ap. J.* 313: 556
Dettmar, R. J., Heithausen, A. 1989. *Ap. J. Lett.* 344: L61
Devereux, N., Young, J. S. 1990a. *Ap. J. Lett.* 350: L25
Devereux, N., Young, J. S. 1990b. *Ap. J.* 359: 42
Devereux, N., Young, J. S. 1991. *Ap. J.* (April 20). In press
Devereux, N., Young, J., Kenney, J. 1991. *Astron. J.* Submitted
Dickman, R. L., Snell, R., Schloerb, F. P. 1986. *Ap. J.* 309: 326
Dopita, M. A. 1985. *Ap. J. Lett.* 295: L5
Draine, B. T., Lee, H. M. 1984. *Ap. J.* 285: 89
Elmegreen, B. G. 1989. *Ap. J.* 338: 178
Elmegreen, B., Elmegreen, D. 1982. *Astron. J.* 87: 626
Elmegreen, B. G., Elmegreen, D. M., Morris, M. 1980. *Ap. J.* 240: 455
Encrenaz, P. J., Stark, A. A., Combes, F., Wilson, R. W. 1979. *Astr. Ap.* 78: L1
Frerking, M., Langer, W., Wilson, R. 1982. *Ap. J.* 262: 590
Gallagher, J. S., Hunter, D. A., Tutukov, A. V. 1984. *Ap. J.* 284: 544
Garcia-Burillo, S., Guelin, M. 1990. In *Dynamics of Galaxies and Molecular Cloud Distribution*, ed. F. Combes, F. Casoli. Dordrecht: Reidel
Garman, L., Young, J. S. 1986. *Astr. Ap.* 154: 8
Gerin, M., Nakai, N., Combes, F. 1988. *Astr. Ap.* 203: 44

Giovanelli, R., Haynes, M. P. 1983. *Astron. J.* 88: 881
Gordon, M. 1991. *Ap. J.* (April 20). In press
Guelin, M., Garcia-Burillo, S., Blundell, R., Cernicharo, J., Despois, D., Steppe, H. 1988. *Highlights Astron.* Vol. 8
Gusten, R., Mezger, P. 1982. *Vistas Astron.* 26: 159
Handa, T., Nakai, N., Sofue, Y., Hayashi, M., Fujimoto, M. 1990. *Publ. Astron. Soc. Jpn.* 42: 1
Hayashi, M., Handa, T., Sofue, Y., Hasegawa, T., Nakai, N., Lord, S. D., Young, J. S. 1987. In *IAU Symp. No. 115, Star Forming Regions*, ed. M. Peimbert, J. Jagaku. Dordrecht: Reidel
Heckman, T., Beckwith, S., Blitz, L., Skrutskie, M., Wilson, A. 1986. *Ap. J.* 305: 157
Heckman, T., Blitz, L., Wilson, A., Armus, L., Miley, G. 1989. *Ap. J.* 342: 735
Hernquist, L. 1989. *Nature* 340: 687
Hildebrand, R. H. 1983. *Q. J. R. Astron. Soc.* 24: 267
Ho, P. T. P., Turner, J. L., Martin, R. N. 1987. *Ap. J. Lett.* 322: L67
Huchtmeier, W., Bregman, J., Hogg, D., Roberts, M. S. 1988. *Astr. Ap.* 198: L17
Huchtmeier, W., Richter, O.-G., Bohnenstengel, H.-D., Hauschildt, M. 1983. In *A General Catalog of HI Observations of External Galaxies.* ESO Preprint No. 250
Huntcr, D. A., Thronson, H., Cascy, S., Harper, D. 1989. *Ap. J.*, 341: 697
Hurt, R., Turner, J. L. 1991. *Ap. J.* In press
Ichikawa, T., Nakano, M., Tanaka, Y. D. 1987. In *IAU Symp. No. 115, Star Forming Regions*, ed. M. Peimbert, J. Jugaku. Dordrecht: Reidel
Ishiguro, M., Kawabe, R., Morita, K.-I., Okumura, S. K., Chikada, Y., et al 1989. *Ap. J.* 344: 763
Ishizuki, S., Kawabe, R., Ishiguro, M., Okumura, S. K., Morita, K.-I., et al 1990. *Nature* 344: 224
Ishizuki, S., Kawabe, R., Ishiguro, M., Okumura, S. K., Morita, K.-I., et al 1990b. *Ap. J.* 355: 436
Israel, F., DeGraauw, T., Van de Stadt, H., DeVries, C. 1986. *Ap. J.* 303: 186
Israel, F., van Dishoeck, E. F., Baas, F., Koornneff, J., Black, J. H., de Graauw, T. 1990. *Astr. Ap.* 227: 342
Jackson, J., Ho, P. T. P. 1988. *Ap. J. Lett.* 324: L5
Jackson, J., Snell, R., Ho, P., Barrett, A. 1989. *Ap. J.* 337: 680
Johansson, L., Booth, R. 1987. In *IAU Symp. No. 115, Star Forming Regions*, ed. M. Peimbert, J. Jugaku. Dordrecht: Reidel
Kaneko, N., Morita, K., Fukui, Y., Sugitani, K., Iwata, T., et al. 1989. *Ap. J.* 337: 691
Kawara, K., Taniguchi, Y., Nakai, N., Sofue, Y. 1990. *Ap. J. Lett.* 365: L1
Kenney, J. 1987. PhD thesis, Univ. Massachusetts, Amherst
Kenney, J., Scoville, N., Wilson, C. 1991. *Ap. J.* In press
Kenney, J., Lord, S. 1991. *Ap. J.* Submitted
Kenney, J., Young, J. 1986. *Ap. J. Lett.* 301: L13
Kenney, J., Young, J. 1988a. *Ap. J. Suppl.* 66: 261
Kenney, J., Young, J. 1988b. *Ap. J.* 326: 588
Kenney, J., Young, J. 1989. *Ap. J.* 344: 171
Kenney, J., Young, J., Hasegawa, T., Nakai, N. 1990. *Ap. J.* 353: 460
Kennicutt, R. C. Jr., Kent, S. M. 1983. *Astron. J.* 88: 1094
Kennicutt, R. C. Jr., Keel, W., van der Hulst, J. M., Hummel, E., Roettiger, K. 1987. *Astron. J.* 93: 1011
Knapp, G. R., Phillips, T. G., Huggins, P. J., Leighton, R. B., Wannier, P. 1980. *Ap. J.* 240: 60
Knezek, P., Young, J. S. 1989. In *2nd Teton Conf. on Interstellar Medium in Galaxies*, ed. H. Thronson, M. Shull. Dordrecht: Kluwer
Krause, M., Cox, P., Garcia-Barreto, J. A., Downes, D. 1990. In *IAU Symp. No. 146, Dynamics of Galaxies and Molecular Cloud Distribution*, ed. F. Combes, F. Casoli. Dordrecht: Reidel.
Kronberg, P. P., Biermann, P., Schwab, F. R. 1985. *Ap. J.* 291: 693
Krugel, E., Steppe, H., Chini, R. 1990. *Astr. Ap.* 229: 17
Kutner, M. L., Ulich, B. L. 1981. *Ap. J.* 250: 341
Lada, C. J., Margulis, M., Sofue, Y., Nakai, N., Handa, T. 1988. *Ap. J.* 328: 143
Larson, R. 1987. In *Galactic and Extragalactic Star Formation*, ed. M. Fich, R. Pudritz
Larson, R., Tinsley, B. 1978. *Ap. J.* 219: 46
Lazareff, B., Castets, A., Kim, D., Jura, M. 1989. *Ap. J. Lett.* 336: L134
Lo, K. Y., Berge, G., Claussen, M., Heiligman, G., Leighton, C., et al. 1984. *Ap. J. Lett.* 282: L59
Lo, K. Y., Ball, R., Masson, C., Phillips, T., Scott, S., Woody, D. 1987a. *Ap. J.* 317: L63
Lo, K. Y., Cheung, K., Masson, C., Phillips, T., Scoville, N., Woody, D. 1987b. In *IAU Symp. No. 115, Star Forming Regions*, ed. M. Peimbert, J. Jugaku. Dordrecht: Reidel
Loiseau, N., Reuter, H.-P., Wielebinski, R., Klein, U. 1988. *Astr. Ap.* 200: L1
Lonsdale, C. J., Helou, G., Good, J. C., Rice, W. L. 1985. *Catalogued Galaxies and Quasars Observed in the IRAS Survey.* Washington, D.C.: US GPO

Lonsdale, C., Persson, E., Matthews, K. 1984. *Ap. J.* 287: 95
Lord, S. D. 1987. PhD thesis, Univ. Mass.
Lord, S. D., Young, J. S. 1990. *Ap. J.* 356: 135
Maloney, P., Black, J. 1988. *Ap. J.* 325: 389
Mauersberger, R., Schulz, A., Baars, J. W. M., Steppe, H. 1990. In *IAU Symp. No. 146, Dynamics of Galaxies and Molecular Cloud Distribution*, ed. F. Combes, F. Casoli. Dordrecht: Reidel
Meixner, M., Puchalsky, R., Blitz, L., Wright, M., Heckman, T. 1990. *Ap. J.* 354: 158
Mezger, P. G. 1978. *Astr. Ap.* 70: 565
Mihalas, D., Binney, J. 1981. *Galactic Astronomy*. New York: W. H. Freeman
Mirabel, F., Booth, R., Garay, G., Johansson, L., Sanders, D. 1988b. *Astr. Ap.* 206: L20
Mirabel, F., Kazes, I., Sanders, D. 1988a. *Ap. J. Lett.* 324: L39
Mirabel, F., Sanders, D. B. 1989. *Ap. J. Lett.* 340: L53
Morris, M., Lo, K. Y. 1978. *Ap. J.* 223: 803
Morris, M., Rickard, L. J. 1982. *Annu. Rev. Astr. Astrophys.* 20: 517
Myers, S. T., Scoville, N. Z. 1987. *Ap. J. Lett.* 312: L39
Nakai, N., Hayashi, M., Handa, T., Sofue, Y., Hasegawa, T., Sasaki, M. 1987. *Publ. Astron. Soc. Jpn.* 39: 685
Nakai, N., et al. 1989
Noguchi, M., Ishibashi, S. 1986. *MNRAS* 219: 305
Norman, C. A., Scoville, N. Z. 1988. *Ap. J.* 332: 124
Ohta, K., Sasaki, W., Saito, M. 1986. *Publ. Astron. Soc. Jpn.* 38: 677
Ohta, K., Sasaki, W., Saito, M. 1988. *Publ. Astron. Soc. Jpn.* 40: 653
Olofsson, H., Rydbeck, G. 1984. *Astr. Ap.* 136: 17
Olsen, K., Kwan, J. 1990. *Ap. J.* 361: 426
Pagel, B. E. J., Edmunds, M. G. 1981. *Annu. Rev. Astr. Astrophys.* 19: 77
Phillips, T. G., Ellison, B. N., Keene, J. B., Leighton, R. B., Howard, R. J., et al. 1987. *Ap. J. Lett.* 322: L73
Phillips, J. P., Mampaso, A. 1989. *Astr. Ap.* 218: 24
Planesas, P., Gomez-Gonzales, J., Martin-Pintado, J. 1989. *Astr. Ap.* 216: 1
Planesas, P., Scoville, N. Z., Myers, S. T. 1991. *Ap. J.* 369: 364
Rand, R., Kulkarni, S. 1990. *Ap. J. Lett.* 349: L43
Rand, R., Tilanus, R. P. J. 1990. In *The Interstellar Medium in Galaxies*, ed. H. A. Thronson, J. M. Shull, p. 525. Dordrecht: Kluwer
Rengarajan, T. N., Verma, R. P. 1986. *Astr. Ap.* 165: 300
Richmond, M. W., Knapp, G. R. 1986. *Astron. J.* 91: 517
Rickard, L., Palmer, P., Morris, M., Zuckerman, B., Turner, B. 1975. *Ap. J. Lett.* 199: L75
Rickard, L. J., Blitz, L. 1985. *Ap. J. Lett.* 292: L57
Rickard, L. J., Harvey, P. M. 1984. *Ap. J. Lett.* 268: L7
Rickard, L. J., Palmer, P. 1981. *Astr. Ap.* 102: L13
Rickard, L., Turner, B., Palmer, P. 1977. *Ap. J. Lett.* 218: L51
Roberts, M. S. 1969. *Astron. J.* 74: 859
Roberts, W. W. Jr., Huntley, J. M., van Albada, G. D. 1979. *Ap. J.* 233: 67
Rots, A. H., Bosma, A., van der Hulst, J. M., Athansoula, E., Crane, P. C. 1990. *Astron. J.* 100: 387
Rowan-Robinson, M., Phillips, T., White, G. 1980. *Astr. Ap.* 82: 381
Rubin, V. C., Burstein, D., Ford, W. K., Thonnard, N. 1985. *Ap. J.* 289: 81
Rubin, V. C., Ford, W. K. Jr., D'Odrico, S. 1970. *Ap. J.* 160: 801
Rubio, M., Garay, G., Montani, J., Thaddeus, P. 1991. *Ap. J.* In press
Rydbeck, G., Hjalmarson, A., Rydbeck, O. E. H. 1985. *Astr. Ap.* 144: 282
Ryden, B., Stark, A. A. 1986. *Ap. J.* 305: 823
Sage, L. 1989. *Ap. J.* 344: 200
Sage, L., Solomon, P. M. 1987. *Ap. J. Lett.* 321: L103
Sage, L., Solomon, P. M. 1989. *Ap. J.* 342: L15
Sage, L., Wrobel, J. 1989. *Ap. J.* 344: 204
Sandage, A. 1986. *Astr. Ap.* 161: 89
Sandage, A., Tammann, G. A. 1981. *The Revised Shapley-Ames Catalog*. Washington, D.C.: Carnegie Inst. RSA
Sanders, D. B. 1990. In *IAU Symp. No. 146, Dynamics of Galaxies and Molecular Clouds Distribution*, ed. F. Combes, F. Casoli. Dordrecht: Reidel
Sanders, D. B., Mirabel, I. F. 1985. *Ap. J.* 298: L31
Sanders, D., Scoville, N. Z., Sargent, A. I., Soifer, B. T. 1988a. *Ap. J. Lett.* 324: L55
Sanders, D., Scoville, N., Soifer, B. T. 1988b. *Ap. J.* 335: L1
Sanders, D. B., Scoville, N. Z., Soifer, B. T. 1991. *Ap. J.* In press
Sanders, D., Scoville, N., Young, J., Soifer, T., Danielson, G. 1986. *Ap. J. Lett.* 305: L45
Sanders, D. B., Scoville, N. Z., Zensus, A., Soifer, B. T., Wilson, T. L., et al. 1989. *Astr. Ap.* 213: L5
Sanders, D. B., Soifer, B. T., Elias, J. H., Madore, B. J., Matthews, K., Neugebauer, G., Scoville, N. Z. 1988c. *Ap. J.* 325: 74

Sanders, D. B., Solomon, P. M., Scoville, N. Z. 1984. *Ap. J.* 276: 182
Sanders, D. B., Young, J., Scoville, N., Soifer, T., Danielson, G. 1987. *Ap. J. Lett.* 312: L5
Sanders, R. H., Huntley, J. M. 1976. *Ap. J.* 209: 53
Sandquist, A., Elfhag, T., Jorsater, S. 1988. *Astr. Ap.* 201: 223
Sandquist, A. A., Elfhag, T., Lindblad, P. O. 1990. *Astr. Ap.* 218: 39
Sargent, A. I., Sanders, D. B., Phillips, T. G. 1989. *Ap. J. Lett.* 346: L9
Sargent, A. I., Sanders, D. B., Scoville, N. Z., Soifer, B. T. 1987. *Ap. J. Lett.* 312: L35
Sargent, A. I., Scoville, N. Z. 1991. *Ap. J. Lett.* 366: L1
Sasaki, M., Ohta, K., Saito, M. 1990. *Publ. Astron. Soc. Jpn.* 42: 361
Scalo, J. 1987. In *Galactic and Extragalactic Star Formation*, ed. M. Fich, R. Pudritz
Scoville, N. Z., Good, J. 1989. *Ap. J.* 339: 149
Scoville, N., Matthews, K., Carico, D., Sanders, D. 1988. *Ap. J. Lett.* 327: L61
Scoville, N. Z., Sanders, D. B. 1987. In *Interstellar Processes*, ed. D. Hollenbach, H. Thronson, p. 21. Dordrecht: Reidel
Scoville, N. Z., Sanders, D. B., Clemens, D. 1986a. *Ap. J. Lett.* 310: L77
Scoville, N. Z., Sanders, D., Sargent, A., Soifer, T., Scott, S., Lo, K. Y. 1986b. *Ap. J.* 311: L47
Scoville, N. Z., Sargent, A. I., Sanders, D. B., Soifer, B. T. 1991. *Ap. J. Lett.* 366: L5
Scoville, N., Sanders, D., Sargent, A., Soifer, T., Tinney, C. 1989. *Ap. J. Lett.* 345: L25
Scoville, N. Z., Soifer, B. T. 1991. In *Massive Stars and Starburst*, ed. K. Leitherer. Cambridge: Cambridge Univ. Press.
Scoville, N. Z., Soifer, B. T., Neugebauer, G., Young, J. S., Matthews, K., Yerka, J. 1985. *Ap. J.* 289: 129
Scoville, N. Z., Young, J. S. 1983. *Ap. J.* 265: 148
Scoville, N. Z., Young, J. S., Lucy, L. B. 1983. *Ap. J.* 270: 443
Scoville, N., Yun, M., Clemens, D., Sanders, D., Waller, W. 1987. *Ap. J. Suppl.* 63: 821
Searle, L., Sargent, W. L. W., Bagnuolo, W. 1973. *Ap. J.* 179: 427
Shaya, E., Federman, S. 1987. *Ap. J.* 319: 76
Silk, J. 1987. In *Galactic and Extragalactic Star Formation*, ed. M. Fich, R. Pudritz, Dordrecht: Kluwer
Sofue, Y. 1988. In *Molecular Clouds in the Milky Way and External Galaxies*, ed. R. Dickman, R. Snell, J. Young. Berlin: Springer-Verlag
Sofue, Y., Doi, M., Ishizuki, N., Nakai, N., Handa, T. 1988. *Proc. Astron. Soc. Jpn.* 40: 511
Sofue, Y., Doi, M., Krause, M., Nakai, N., Handa, T. 1989a. *Proc. Astron. Soc. Jpn.* 41: 113
Sofue, Y., Hasegawa, T., Nakai, N., Handa, T., Hayashi, M. 1986. *Proc. Astron. Soc. Jpn.* 38: 161
Sofue, Y., Handa, T., Nakai, N. 1989b. *Proc. Astron. Soc. Jpn.* 41: 937
Sofue, Y., Nakai, N., Handa, T. 1987. *Proc. Astron. Soc. Jpn.* 39: 47
Sofue, Y., Taniguchi, Y., Handa, T., Wakamatsu, K., Nakai, N., et al. 1990. *Proc. Astron. Soc. Jpn.* 42: L45
Solomon, P. M. 1982. In *Greenbank Workshop on Extragalactic Molecules*, ed. L. Blitz
Solomon, P. M., Barrett, J., Sanders, D. B., de Zafra, R. 1983. *Ap. J. Lett.* 266: L103
Solomon, P. M., de Zafra, R. 1975. *Ap. J. Lett.* 199: L79
Solomon, P. M., Radford, S. J. E., Downes, D. 1990. *Ap. J. Lett.* 348: L53
Solomon, P. M., Sage, L. 1988. *Ap. J.* 334: 613
Solomon, P. M., Rivolo, R., Barrett, J., Yahil, A. 1987. *Ap. J.* 319: 730
Solomon, P. M., Sanders, D. B., Rivolo, A. R. 1985. *Ap. J. Lett.* 292: L19
Solomon, P. M., Scoville, N. Z., Sanders, D. B. 1979. *Ap. J. Lett.* 232: L89
Spitzer, L. 1978. In *Physical Processes in the Interstellar Medium*, p. 162. New York: Wiley-Interscience
Stanford, S. A., Sargent, A. I., Sanders, D. B., Scoville, N. Z. 1990. *Ap. J.* 349: 492
Stark, A. A. 1979. PhD thesis, Princeton Univ.
Stark, A. A. 1983. In *Kinematics, Dynamics, and Structure of the Milky Way*, ed. W. Shuter, p. 127. Dordrecht: Reidel
Stark, A. A., Carlson, E. R. 1984. *Ap. J.* 279: 122
Stark, A., Elmegreen, B., Chance, D. 1987. *Ap. J.* 322: 64
Stark, A. A., Knapp, G. R., Bally, J., Wilson, R. W., Penzias, A. A., Rowe, H. 1986. *Ap. J.* 310: 660
Sutton, E., Masson, C., Phillips, T. G. 1983. *Ap. J.* 275: L49
Tacconi, L. 1987. PhD thesis, Univ. Mass.
Tacconi, L., Young, J. S. 1985. *Ap. J.* 290: 602
Tacconi, L., Young, J. S. 1986. *Ap. J.* 308: 600
Tacconi, L., Young, J. S. 1987. *Ap. J.* 322: 681
Tacconi, L., Young, J. S. 1989. *Ap. J. Suppl.* 71: 455
Tacconi, L., Young, J. S. 1990. *Ap. J.* 352: 595

Taniguchi, Y., Kameya, O., Nakai, N., Kawara, K. 1990a. *Ap. J.* 358: 132
Taniguchi, Y., Sofue, Y., Wakaimatsu, K., Nakai, N. 1990b. *Ap. J.* 100: 1086
Telesco, C. M., Campins, H., Joy, M., Dietz, K., Decher, R. 1990. *Ap. J.* Submitted
Telesco, C. M., Harper, D. A. 1980. *Ap. J.* 235: 392
Thronson, H., Tacconi, L., Kenney, J., Greenhouse, M., Margulis, M., et al. 1989b. *Ap. J.* 344: 747
Thronson, H., Hereld, M., Majewski, S., Greenhouse, M., Johnson, P., et al. 1989c. *Ap. J.* 343: 158
Thronson, H., Hunter, D., Casey, S., Latter, W., Harper, D. 1989a. *Ap. J.* 339: 803
Thronson, H., Hunter, D. A., Telesco, C. M., Greenhouse, M., Harper, D. A. 1988. *Ap. J.* 344: 605
Thronson, H., Hunter, D. A., Telesco, C. M., Harper, D. A., Decher, R. 1987. *Ap. J.* 317: 180
Tilanus, R. P. J., Tacconi, L. J., Zhu, S., Sanders, D. B., Sutton, E. C., et al. 1991. *Ap. J. Lett.* In press
Tinney, C. G., Scoville, N. Z., Sanders, D. B., Soifer, B. T. 1990. *Ap. J.* 362: 473
Toomre, A., Toomre, J. 1972. *Ap. J.* 178: 623
Turner, J., Martin, B., Ho, P. T. P. 1990. *Ap. J.* 351: 418
van Driel, W. 1987. PhD thesis, Univ. Groningen
van Gorkom, J., Kotanyi, C. 1985. In *ESO Workshop on the Virgo Cluster of Galaxies*, ed. O.-G. Righter, B. Binggeli, p. 61. Garching: ESO
Verter, F. 1983. PhD thesis, Princeton Univ.
Verter, F. 1987. *Ap. J. Suppl.* 64: 555
Verter, F. 1988. *Ap. J. Suppl.* 68: 129
Vogel, S., Boulanger, F., Ball, R. 1987. *Ap. J. Lett.* 316: 243
Vogel, S., Kulkarni, S., Scoville, N. 1988. *Nature* 334: 402
Wall, W. F., Jaffe, D. T. 1990. *Ap. J. Lett.* 361: L45
Wang, Z. 1990. *Ap. J.* 360: 529
Warmels, R. H. 1986. PhD thesis, Groningen
Weliachew, L., Casoli, F., Combes, F. 1988. *Astr. Ap.* 199: 353
Wevers, B., van der Kruit, P., Allen, R. 1986. *Astr. Ap. Suppl.* 55: 505
Whiteoak, J. B., Dahlem, M., Wielebinski, R., Harrett, J. I. 1990. *Astr. Ap.* 231: 25
Wiklind, T., Henkel, C. 1989. *Astr. Ap.* 225: 1
Wiklind, T., Henkel, C. 1990. *Astr. Ap.* 227: 394
Wiklind, T., Rydbeck, G., Hjalmarson, A., Bergman, P. 1990. *Astron. Astrophys.* 232: L11
Wiklind, T., Rydbeck, G., Hjalmarson, A., Rydbeck, O. 1987. In *IAU Symp. No. 115, Star Forming Regions*, ed. M. Peimbert, J. Jugaku. Dordrecht: Reidel
Wild, W., Eckart, A., Genzel, R., Harris, A., Jackson, J., et al. 1989. In *2nd Teton Conf. on Interstellar Medium in Galaxies*, ed. H. Thronson, M. Shull, Dordrecht: Kluwer
Wilson, C., Reid, M. 1991. *Ap. J. Lett.* In press
Wilson, C., Scoville, N. 1989. *Ap. J.* 347: 743
Wilson, C., Scoville, N. Z. 1990. *Ap. J.* In press
Wilson., T., Fricke, K., Biermann, P. 1979. *Astr. Ap.* 79: 245
Wyse, R. 1986. *Ap. J. Lett.* 311: L41
Wyse, R., Silk, J. 1989. *Ap. J.* 339: 700
Young, J. S. 1987. In *IUA Symp. No. 115, Star Forming Regions*, ed. M. Peimbert, J. Jugaku. Dordrecht: Reidel
Young, J. S. 1990. In *The Interstellar Medium in Galaxies*, ed. H. Thronson, M. Shull. Dordrecht: Kluwer
Young, J. S., Claussen, M., Scoville, N. 1988a. *Ap. J.* 324: 115
Young, J. S., Devereux, N. A. 1991. *Ap. J.* In press
Young, J. S., Gallagher, J. S., Hunter, D. A. 1984a. *Ap. J.* 276: 476
Young, J. S., Kenney, J., Lord, S., Schloerb, F. P. 1984b. *Ap. J. Lett.* 287: L65
Young, J. S., Claussen, M., Kleinmann, S. G., Rubin, V., Scoville, N. 1988b. *Ap. J. Lett.* 331: L81
Young, J. S., Knezek, P. 1989. *Ap. J. Lett.* 347: L55
Young, J. S., Kenney, J., Tacconi, L., Claussen, M., Huang, Y.-L., et al. 1986b. *Ap. J. Lett.* 311: L17
Young, J. S., et al. 1991. *Ap. J.* Submitted
Young, J. S., Sanders, D. B. 1986. *Ap. J.* 302: 680
Young, J. S., Schloerb, F. P., Kenney, J., Lord, S. D. 1986a. *Ap. J.* 304: 443
Young, J. S., Scoville, N. Z. 1982a. *Ap. J.* 258: 467
Young, J. S., Scoville, N. Z. 1982b. *Ap. J. Lett.* 260: L11
Young, J. S., Scoville, N. Z. 1982c. *Ap. J. Lett.* 260: L41
Young, J. S., Scoville, N. Z. 1984. *Ap. J.* 287: 153
Young, J. S., Scoville, N. Z., Brady, E. 1985. *Ap. J.* 288: 487
Young, J. S., Tacconi, L., Scoville, N. Z. 1983. *Ap. J.* 269: 136
Young, J. S., Xie, S., Kenney, J., Rice, W. L. 1989. *Ap. J. Suppl.* 70: 699

Annual Review of Astronomy and Astrophysics
Volume 29, 1991

CONTENTS